Development of novel anti-cancer strategies utilizing the zebrafish xenograft model

Chen, Q.

Chapter 5

Light triggered, cancer cell-specific targeting and liposomal drug delivery in a zebrafish xenograft model

Li Kong[1]⊥, Quanchi Chen[2]⊥, Frederick Campbell[1], Ewa Snaar-Jagalska[2]* and Alexander Kros[1]*

⊥ Authors contributed equally

[1]Supramolecular and Biomaterials Chemistry, Leiden Institute of Chemistry, Leiden University, Einsteinweg 55, 2333 CC Leiden, The Netherlands

[2]Institute of Biology, Leiden University, Leiden 2311 EZ, The Netherlands

E-mail: a.kros@chem.leidenuniv.nl, b.e.snaar-jagalska@biology.leidenuniv.nl

Published in: Advanced Healthcare Materials 2020, 9, 1901489; doi: 10.1002

Keywords: cancer nanomedicine, liposomes, light activation, *in vivo,* embryonic zebrafish

Abstract

Cell-specific drug delivery remains a major unmet challenge for cancer nanomedicines. Here, we demonstrate light-triggered, cell-specific delivery of liposome-encapsulated doxorubicin to xenograft human cancer cells in live zebrafish embryos. Our method relies on light triggered dePEGylation of liposome surfaces to reveal underlying targeting functionality. To demonstrate general applicability of our method, we show light triggered, MDA-MB-231 breast cancer cell specific targeting *in vivo* (embryonic zebrafish) using both clinically relevant, folate-liposomes, as well as an experimental liposome-cell fusion system. In the case of liposome-cell fusion, delivery of liposomal doxorubicin direct to the cytosol of target cancer cells resulted in enhanced cytotoxicity, compared to doxorubicin delivery *via* either folate-liposomes or free doxorubicin, as well as a significant reduction in xenograft cancer cell burden within the embryonic fish.

Introduction

The majority (5 of 7) of clinically approved, *targeted* nanomedicines are liposomal formulations used to treat various human cancers [1,2]. All function through passive targeting of solid tumors *via* the enhanced permeability and retention (EPR) effect – a phenomenon characterized by the ill-defined ("leaky") vasculature and poor lymphatic drainage of select solid tumors [3,4]. To maximize passive targeting to solid tumors, PEGylation of nanoparticle surfaces is a long-standing strategy to reduce serum protein absorption, limit nanoparticle recognition and clearance by the reticulo-endothelial system (RES) in the liver and spleen, and prolong circulation lifetimes [5,6]. Once passively accumulated within the target tumor, however, drugs must be released from a nanoparticle at effective therapeutic concentrations (typically cytotoxic concentrations). In the case of Doxil® (PEGylated liposomal doxorubicin) – the first clinically approved, targeted cancer nanomedicine – extracellular drug release relies on passive diffusion of doxorubicin across the liposome membrane. To maximise free drug concentrations within targeted tumors, methods to actively load very high concentrations of doxorubicin within liposomes have been developed [7]. Despite this, the superiority of clinically approved liposomal doxorubicin formulations, over administered free doxorubicin, remains contentious. It is now generally accepted that improved toxicological profiles, rather than improved efficacy, constitute the main pharmacological benefit of liposomal-doxorubicin formulations (over administration of the free drug).

A potentially more effective strategy to treat cancer is to promote cellular uptake of drug-filled nanomedicines within cancer cells. This is most commonly attempted through the display of active targeting moieties (e.g. RGD, folate) from a nanoparticle surface [8,9]. However, active targeting strategies to promote cellular uptake of nanoparticles typically conflict with strategies employed to prolong circulation lifetimes. Most notably, the extremely limited cellular uptake of PEGylated nanoparticles hinders efficient intracellular drug delivery to cancer cells [10]. To overcome this PEG

dilemma, stimuli-responsive dePEGylation of nanoparticles within the target tumor has been investigated [11,12]. In the majority of cases, dePEGylation is triggered by an endogenous stimuli (low pH [13], matrix metalloproteinases [14]), exploiting pathophysiological differences between healthy and tumor tissues. However, suboptimal cleavage conditions/rates – common pH-sensitive groups (*e.g.* hydrazones, acetals and benzoic imines) are optimally sensitive at pH <6, whereas the tumor microenvironment is generally pH >6.5 [15]– typically lead to inefficient drug release profiles. Alternatively, dePEGylation of a nanoparticle can be triggered by an external stimuli, *e.g.* light [12]. In this way, nanoparticle activation can be localized with very high spatiotemporal resolution, including deep within tissue. Two photon excitation sources, for example, can be used to focus light within femtoliter (fL) volumes at tissue depths of up to 1 cm [16,17], while deeper tissues/pathologies can be accessed using fibre optic LEDs or injectable microLEDs [18-20]. Although the use of light to dePEGylate nanomedicines has mainly been used to trigger *extracellular* drug release from a nanocarrier [21-26], enhanced tumor targeting and active cellular uptake of dual responsive polymersomes following light activation has recently been reported [27]. In this case, near-infrared (NIR) light was used in combination with upconverting nanoparticles (UCNPs) to achieve efficient nanoparticle dePEGylation deep within a murine xenograft tumor.

Herein, we show light-triggered and cell specific targeting of doxorubicin-filled liposomes to xenograft breast cancer cells in live embryonic zebrafish. Our method relies on responsive dePEGylation of a liposome surface, *in situ* and *in vivo*, to reveal underlying, active targeting functionality tethered to the liposome surface. To demonstrate the general applicability of this approach, we show light-triggered targeting of liposomal-doxorubicin formulations to cancer cells using both clinically relevant, folate-decorated liposomes (F-liposomes, targeting the overexpressed folate receptor on xenograft MDA-MB-231 cells [28,29]), as well as an experimental, two component (peptide E and K) fusion system that promotes direct fusion of liposome and cell membranes, with concurrent cytosolic delivery of encapsulated liposomal content (**Figure 1**) [30]. For the fusion system, liposome-cell interactions rely on the recognition and binding of two coiled-coil forming peptides – peptide E (*amino acid sequence*: $(EIAALEK)_n$) and peptide K (*amino acid sequence*: $(KIAALKE)_n$) – tethered to opposing lipid membranes [31]. For this system to work, target cancer cell membranes must, therefore, first be enriched with the synthetic lipopepetide CPK (cholesterol-PEG_4-peptide K, see **Scheme S1** for chemical structure) to form K-funtionalised cells. Once engrafted *in vivo*, these cells can recognize, bind to and fuse with circulating liposomes whose membranes are enriched with the complementary lipopepetide, CPE (cholesterol-PEG_4-peptide E, see **Scheme S1** for chemical structure). Crucially, prior to light-triggered dePEGylation, both PEGylated E- and PEGylated F-liposomes freely circulated throughout the vasculature of the embryonic fish and did not interact either with xenograft cancer cells or key RES cell types of the embryo.

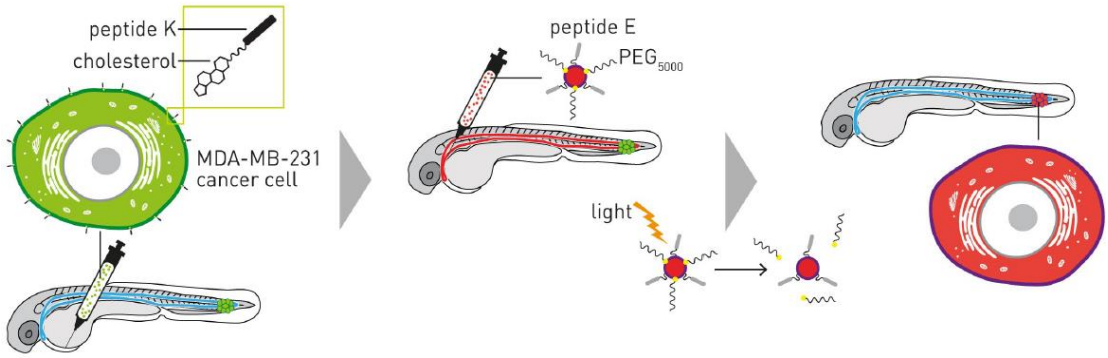

Figure 1 Light-triggered, cancer-cell specific liposome-cell fusion in xenograft zebrafish embryos. Human cancer cells are first pre-functionalised with cholesterol-peptide K4 in vitro. Functionalised cancer cells are then injected into the circulation (via the Duct of Cuvier) of 2-day old zebrafish embryos. Xenograft cancer cells quickly accumulate within the caudal hematopoietic tissue (CHT) of the embryo. One hour after cancer cell injection, EPEG-liposomes are injected into circulation via the posterior caudal vein (PCV). Prior to light triggered dePEGylation, liposomes are confined to the vasculature of the fish and freely circulate. Following UV irradiation and in situ dePEGylation, liposomes rapidly and selectively bind to and fuse with xenograft cancer cells. This interaction is mediated through the recognition of fusogenic peptides E and K displayed from opposing lipid membranes. Liposome-encapsulated cargos (eg. cytotoxic drugs) are delivered directly to the cytosol of the recipient cell.

Materials

1,2-dioleoyl-sn-glycero-3-phosphocholine (DOPC), 1,2-dioleoyl-sn-glycero-3-phosphoethanolamine (DOPE), 1,2-dioleoyl-sn-glycero-3-phosphoethanolamine-N-(7-nitro-2-1,3-benzoxadiazol-4-yl) (DOPE-NBD), 1,2-dioleoyl-sn-glycero-3-phosphoethanolamine-N-(lissamine rhodamine B sulfonyl) (DOPE-LR), 1,2-dipalmitoyl-sn-glycero-3-phosphoethanolamine-N-(6-((folate)amino)hexanoyl) (DPPE-FolateCap) and 1,2-distearoyl-sn-glycero-3-phosphoethanolamine-N-[methoxy(polyethylene glycol)-5000] (ammonium salt) (DSPE-PEG_{5000}) were purchased from Avanti Polar Lipids. 1,2-Dioleoyl-sn-glycero-3-phosphoethanolamine-Atto633 was purchased from ATTO-TEC GmbH (Germany). Cholesterol, doxorubicin hydrochloride (DOX), propidium iodide (PI) and all other chemical reagents were purchased at the highest grade available from Sigma Aldrich and used without further purification. All solvents were purchased from Biosolve Ltd. Phosphate buffered saline (PBS): 5 mM KH_2PO_4, 15 mM K_2HPO_4, 150 mM NaCl, pH 7.4. Lipopeptide constructs – E_4 and K_4 – were synthesized as previously reported [30]. Photolabile cholesterol-PEG constructs – PEG_{2000} and PEG_{5000} – were synthesized as previously reported [32].

Light source

A 375-nm LED (Maximum measured wavelength = 370 nm, FWHM = 13.4 nm; H2A1-H375-S, Roithner Lasertechnik, Vienna, Austria), driven by a custom-built LED driver (I = 350 mA), was used as UV light source in all cases except for Figure S2. Irradiation setups, timings, power densities (as determined by

light actinometry) and light doses (for cell and zebrafish experiments) are reported for individual experiments. For monitoring the photolysis of E_{PEG}-liposomes (Figure S2), UV lamp (SUNON lamp SF9225AT; 56.8 W, 50-60 Hz) was used as UV light source.

Liposome formulation and biophysical characterisation

Phospholipids (DOPC:DOPE:cholesterol; 2:1:1), as a stock solution (10 mM) in chloroform, and either lipopeptide E_4 or K_4, as a stock solution (100 μM) in chloroform:methanol (1:1), or DPPE-Folate as a stock solution (100 μM) in chloroform, were mixed to the desired molar ratios and dried to a film, first under a stream of N_2 and then >1h under vacuum. The lipid film was then re-hydrated in PBS and sonicated (Branson 2510 Ultrasonic Cleaner) for 5 min at 55^{o}C to yield E-liposomes, K-liposomes or F-liposomes respectively (1 mol% E/K/folate in all cases).

Post-modification of E- and F-liposomes with photolabile cholesterol-PEG constructs was carried out as previously described [32]. Briefly, for lipid mixing experiments involving E-liposomes, hydrated and sonicated solutions of cholesterol-PEG (2-20 μM) in PBS were added in equal volumes to E-liposomes (200 μM total [lipid]) in PBS and incubated for 30 min to yield E-liposomes (100 μM total [lipid]) with varying mol% cholesterol-PEG displayed from the outer membrane leaflet. For lipid mixing experiments, fluorescent lipid probes (DOPE-NBD and DOPE-LR, 0.5 mol% each) were included within E-liposome formulations.

Hydrodynamic diameters of all liposomes, as measured by dynamic light scattering (DLS; Zetasizer Nano ZS, Malvern Instruments, UK) were approx. 100 nm and polydispersities <0.2. DLS measurements were made at room temperature and at a total lipid concentration of 100μM. For zeta potential measurements (Zetasizer Nano ZS, Malvern Instruments, UK), liposomes were formulated in ddH_2O and diluted in salt (NaCl) solution. Zeta potentials were measured at room temperature, at 500 μM total lipid concentration and 10mM NaCl concentration. All reported DLS measurements and zeta potentials are the average of three measurements. For DLS and zeta potential experiments monitoring changes following light activation, liposomes were irradiated (370 ± 7 nm, 202 mW/cm^2) for 15 mins in quartz cuvettes with the LED mounted 1 cm from the sample.

For transmission electron microscopy (TEM) images of EPEG-liposomes and FPEG-liposomes, a drop of liposome solution (1 mM) was placed on a lacey carbon covered TEM copper grid for 3 mins before dabbing dry through the underside of the grid with a tissue. The sample was then washed three times with ddH_2O, Finally, a drop of phosphotungstic acid (TPA, 1% w/v) in H_2O was added and the sample left to dry in the dark. Images were obtained at an accelerating voltage of 100 kV (TEM JEOL 1230 instrument).

Propidium iodide encapsulation within E-liposomes

Propidium iodide (PI) was loaded into E-liposomes *via* passive encapsulation. Briefly, lipid films (1 mM total lipids) were hydrated in PBS containing 15 mM PI and sonicated for 2−3 min in a sonication bath at 55 °C. Un-encapsulated PI was removed through size exclusion chromatography (illustra™ NAP™ Sephadex™ G-25, GE-Healthcare, USA) according to the manufacturer's guidelines. *Final concentration for cell experiments*: liposomes (400 µM total lipids); encapsulated PI (75 µM).

Doxorubicin encapsulation within E- and F-liposomes

Active loading of doxorubicin hydrochloride (DOX) was carried out as previously reported [7]. Briefly, liposomes (10mM total lipid) were formulated (sonication) in sodium citrate buffer (pH 3.5) before being passed through a size exclusion column (illustra™ NAP™ Sephadex™ G-25, GE Healthcare, USA) using PBS buffer (pH 7.4) as eluent to set up a pH gradient across the liposome membrane. Next, DOX (powder) was added to the liposomal solution at a final concentration of 1 mg/mL and incubated overnight at 4 °C. Finally, free DOX was removed by size exclusion chromatography (illustra™ NAP™ Sephadex™ G-25, GE Healthcare, USA). The entrapment efficiency (EE) and drug loading content (DL) of DOX was determined using UV−vis spectrophotometry (Cary 300 UV-Vis, Agilent). Briefly, liposomes were solubilized by addition of Triton X-100 (0.5% v/v), absorption measured at 480nm, and [DOX] calculated against a predetermined DOX calibration curve (free DOX in PBS containing Triton X-100 (0.5% v/v). The loading efficiency was calculated according to the following equation:

$$\mathrm{EE} = \frac{\mathrm{C_{DOX\ in\ liposomes}}}{\mathrm{C_{total}}} * 100\%$$

$$\mathrm{DL} = \frac{\mathrm{Weight\ of\ DOX}}{\mathrm{Weight\ of\ liposomes}} * 100\%$$

Where $C_{DOX\ in\ liposomes}$ is the concentration of DOX determined in the liposomes, C_{total} is the total added concentration of DOX, '*Weight of DOX*' is the weight of DOX encapsulated in the liposomes and '*Weight of liposomes*' is the weight of liposomes. Unfortunately, active loading of DOX, in this case, did not yield the high reported encapsulation efficiencies (typically >85%) as expected. After final size exclusion column chromatography, E_{PEG}-liposomes (4 mM total lipid concentration) contained 200 µM DOX (5% EE, 4.02% DL), whereas F_{PEG}-liposomes (4 mM total lipid concentration) contained 195 µM DOX (4.8% EE, 3.92% DL).

DOX concentrations for WST in vitro experiments: liposomal-DOX formulations either diluted or concentrated (spin column) to desired [DOX] – ie. 200 µM DOX = 4 mM total lipids; 50 µM DOX = 1mM total lipids.

NOTE: For F-liposomes, total lipid concentrations (and therefore [folate]) are 2.5% higher than for E-liposomes (and [peptide E]) at identical [DOX] to compensate for the slight variation in EE between E- and F-liposomes.

NOTE: where [DOX] <25 µM and [total lipid] <500 µM, the concentration of peptide E (1mol%, displayed from the liposome surface) is less than the concentration of peptide K (5 µM, displayed from the cell membrane).

Final DOX concentrations for in vivo (zebrafish embryo xenograft) experiments: 200 µM DOX; 4 mM total lipids (40 µM peptide E).

In vitro DOX release

To monitor the release of DOX from liposomes, 1 mL of DOX loaded liposomes (200 µM DOX; 4 mM E_{PEG} liposomes or 4.1 mM F_{PEG} liposomes) in PBS were placed in dialysis tubing (MWCO: 3.5 KDa) and dialyzed against 20 mL PBS at 37°C. At various time intervals, 3.0 mL of dialysis buffer was removed and replaced with fresh buffer. The amount of released DOX was quantified by flurescence emission at 595 nm (Ex = 480 nm) against a predetermined calibration curve (DOX in PBS). The cumulative release was calculated according to the following equation:

$$\text{Cumulative release } (\%) = \frac{\text{C}_{\text{cumulative release}}}{\text{C}_{\text{total}}} \times 100$$

where $C_{cumulative\ release}$ is the cumulative released concentration of DOX in dialysis buffer and C_{total} is the total added concentration of DOX. At each successive timepoint, $C_{cumulative\ release}$ was corrected to account for the removed and replaced dialysis buffer of previous timepoints (eg. $C_{\text{cumulative release (at the 4th time point)}} = 3(C_{\text{DOX at the 1st time point}} + C_{\text{DOX at the 2nd time point}} + C_{\text{DOX at the 3rd time point}}) + 20(C_{\text{DOX at the 4th time point}})$). To monitor light activated release of DOX, liposomes were irradiated (370 ± 7 nm, 202 mW/cm^2) for 15 mins in quartz cuvettes, with the LED mounted 1 cm from the sample, before adding to the dialysis tube.

Photolysis of E_{PEG}-liposomes

A solution of E_{PEG}-liposomes (total lipid = 5 mM, 4 mol% PEG_{5000}, 1 mol% of lipopeptide E_4) in PBS was irradiated under the UV lamp (SUNON UV lamp SF9225AT; 56.8 W, 50-60 Hz), for 5 min, followed immediately by acquisition of the UV-visible absorption spectra. The same sample was then re-irradiated and this cycle repeated for cumulative irradiation time points of 10, 20, 30, 40 and 60 min.

Lipid mixing assay

For lipid mixing assays, NBD fluorescence (excitation: 465 nm emission: 530 nm) was measured upon mixing fluorescent E_{PEG}-liposomes and non-fluorescent K-liposomes every 20 s for 3500 s (TECAN Plate Reader Infinite M1000). The 0% value was determined by measuring NBD emission of E_{PEG}-liposomes

to which an equal amount of PBS (in place of K-liposomes) was added. The 100% value was determined using liposomes containing half the fluorescent probe (DOPE-NBD and DOPE-LR) concentrations ie. 0.25 mol%. The percentage of lipid mixing (%F(t)) was calculated as:

$$\%F(t) = \frac{F(t) - F0}{Fmax - F0}$$

where F(t) is the fluorescence intensity measured, F_0 is the 0% fluorescence intensity and F_{max} is the 100% fluorescence intensity. For measuring the effects of UV irradiation on the rate of lipid mixing, E_{PEG}-liposomes were irradiated liposomes were irradiated (370 ± 7 nm, 202 mW/cm^2) for 15 mins with the LED mounted at a distance of 1 cm from the sample, prior to the addition of K-liposomes.

Cell culture, WST and *in vitro* assays

HeLa cells and MDA-MB-231 breast cancer cells (ATCC), stably expressing GFP (Plasmid #106172; Addgene.org) were cultured in Dulbecco's Modified Eagle's Medium (DMEM)/F12, supplemented with 10% fetal calf serum (FCS, iron supplied), 2% L-glutamine. Cells were cultured in an atmosphere of 5% CO_2 at 37°C. Medium was refreshed every two days and cells passaged at 70% confluence by treatment with trypsin-EDTA (0.05% trypsin).

For *in vitro* assays (Figure 2b), HeLa cells (1x10^5 mL^{-1}) were transferred to 8-well cell culture plates (300 µL, µ-Slide 8 Well, Ibidi GmbH) and cultured for a further 24 h. A solution of lipopeptide K_4 (5 µM in DMEM + 10% FCS; prepared by sonication, 5 min, 55°C, Branson 2510 Ultrasonic Cleaner), was added (300 µL) to cells and incubated for 2 h at 37 °C. The lipopeptide K_4 solution was carefully removed and cells washed (3 x PBS). E_{PEG}-liposomes (300 µL, 400 µM, 8 mol% PEG_{2000} *or* 4 mol% PEG_{5000}, 1mol% DOPE-NBD) in PBS, with encapsulated PI (75 µM), were then added to cells and incubated at 37 °C for 20 min. Cells were then washed (3 x DMEM+FCS) and immediately imaged by confocal microscopy (Leica TCS SP8, Solms, Germany; *wavelengths*: NBD-DOPE: Ex/Em: 455/530 nm (Ex laser: 488 nm), propidium iodide: Ex/Em: 535/617 nm (Ex laser: 543 nm). For light triggered membrane fusion, E_{PEG}-liposomes (300 µL, 400 mM, 4 mol% PEG_{5000}) were added to cells and irradiated (15 mins, 370 ± 7 nm, 50.6 mW/cm^2, *light dose* = 45.5 J/cm^2) from directly above (2cm) the well plate. Following irradiation, cells were incubated for a further 20 min, washed (3 x DMEM+FCS) and imaged. To demonstrate spatial control over liposome-cell membrane fusion, E_{PEG}-liposomes (300 µL, 400 µM, 4 mol% PEG_{5000}) were added cells, the well plate half covered with aluminum foil and irradiation applied as above. Following incubation at 37 °C for 20 min, cells were carefully washed (3 x DMEM+FCS) and confocal imaging performed across the boundary of the (now removed) aluminium foil.

For WST cell proliferation assays, MDA-MB-231 cells were seeded in 96-well plates (10,000 cells per well) and incubated overnight. For E-liposome experiments, lipopeptide-K solution (5 µM, 100 µL,

DMEM+FCS) was added to cells, incubated for 2 h and washed away (3 x PBS). For F-liposomes, cells were simply washed with PBS prior to addition of liposomes. To the cells were then added either solutions of free DOX (100 µL, varying concentrations in 1:1 PBS:DMEM+FCS), E_{PEG}-liposomes or F_{PEG}-liposomes, both containing DOX (100 µL varying liposome/DOX concentrations in 1:1 PBS:DMEM+FCS) and incubated for 2 h. For the '+UV' liposome samples, cells were irradiated (15 mins, 370 ± 7 nm, 50.6 mW/cm^2, *light dose* = 45.5 J/cm^2) immediately after sample addition to cells. Following incubation, cells were washed (3 x DMEM+FCS), re-suspended in DMEM+FCS and incubated for a further 24 h. Cell media was then removed and 100 µL Cell Proliferation Reagent, WST-1 (Sigma) added to each well. Cells were incubated for a further 3 h, according to the supplier guidelines. To determine cell viability, absorbance at 450 nm was measured. All experiments were carried out in quadruplicate.

Zebrafish experiments

Zebrafish (Danio rerio, strain AB/TL) were maintained and handled according to the guidelines from the Zebrafish Model Organism Database (http://zfin.org) and in compliance with the directives of the local animal welfare committee of Leiden University. Fertilization was performed by natural spawning at the beginning of the light period, and eggs were raised at 28.5 °C in egg water (60 µg/mL Instant Ocean sea salts). At 24 hours post-fertilization (hpf), 0.2 mM N-phenylthiourea was added to the egg water to prevent malanization. At 2 days post-fertilisation (dpf), embryos were anaesthetized with 0.01% tricaine and embedded in 0.4% agarose containing tricaine prior to microinjection. In addition to WT embryos, the established zebrafish line *Tg(*kdrl:GFP/mpeg1:GAL4^{gl24}/UAS-E1b:nfsB-mCherry^{i149}) [33] was also used (Figure 3a).

For biodistribution studies in zebrafish embryos, MDA-MB-231 cells (2 x 10^6) were suspended in (PBS/EDTA), pelleted (5 min, 1200 rpm), washed (PBS), pelleted again and finally re-suspended in 2% PVP in PBS (10 µL) ready for injection. Suspended cells were loaded in a glass capillary needle, prepared using a Flaming/Brown micropipette puller (model P-99, HEAT=496, PULL=95, VEL.=60, TIME=90, Sutter Instrument Co.) Forceps were used to cut the end of the needles and the exposure time and gas pressure were adjusted in order to inject around 300 cells. Cells were engrafted into the circulation of a 2-day old embryo, *via* the Duct of Cuvier. In the case of E-liposome experiments, MDA-MB 231 cells were pretreated with lipopeptide-K, as for *in vitro* assays. One hour after engraftment, E_{PEG}- or F_{PEG}-liposomes (1 mM, 3 nL, 4mol% PEG_{5000}, 1mol% DOPE-LR) in PBS were injected into circulation *via* the posterior cardinal vein. Embryos were kept at 34 °C. For *in situ* UV irradiation (15 mins, 370 ± 7 nm, 13.5 mW/cm^2, *light dose* = 0.45 J/embryo), the LED light source was positioned directly above (3 cm) the embryo in agarose. Images were taken 45 min after liposome injection using either a Leica MZ16FA fluorescent microscope coupled to a DFC420C camera or Leica TCS SPE confocal microscope. Wavelength settings for GFP Ex: 488 nm, Em: 500-550 nm and for rhodamine Ex laser: 552 nm, Ex laser: 570-650 nm. Images were processed and quantified using the Fiji distribution of ImageJ [34].

For doxorubicin delivery in zebrafish embryos, 3 nL doxorubicin-filled E_{PEG}-liposomes (4 mM total lipids, 4 mol% PEG_{5000}, 200 µM DOX) in PBS were injected into the circulation of 2-day old xenograft zebrafish embryos (K-functionalised MDA-MB-231 cells, generated as described above) *via* the posterior cardinal vein. Embryos were kept at 34 °C throughout the course of the experiment. Where applicable, UV irradiation (15 mins, 370 ± 7 nm, 13.5 mW/cm^2, *light dose* = 0.45 J/embryo) was performed immediately following liposomes injection. The LED light source was positioned directly above (3 cm) the embryo in agarose. Four days post-injection (4 dpi), fluorescent images were obtained, using a Leica MZ16FA fluorescent microscope coupled to a DFC420C camera and Leica TCS SPE confocal microscope, and cancer cell mass, within the tail invasive site, quantified based on the green fluorescent signal of xenograft MDA-MB-231 cells (Image analysis software: ImageJ 1.51n, National Institutes of Health, USA). One-way ANOVA tests were performed to compare means of the three groups of data.

Statistical Analysis

Data presented as mean values ± SD. No pre-processing of data was performed. Data was analysed by one-way ANOVA (non-parametric and mixed) statistical test using GraphPad Prism 8.0.1. Significance is shown as P value (****, $p < 0.0001$; NS, not significant). Sample sizes for each statistical analysis are individually reported and no statistical methods were used to predetermine sample size.

Results and Discussion

We have previously shown the interaction between fusogenic peptides E and K, displayed from opposing membranes, can be sterically shielded through PEGylation of E-functionalized liposomes (E_{PEG}-liposomes) [35]. Furthermore, through incorporation of a photocleavable linker, we have shown precise spatiotemporal control of liposome-liposome fusion and liposome-cell docking through light triggered dePEGylation of E_{PEG}-liposomes *in vitro* [32]. In this case, PEG_{2000} was sufficient in length to sterically shield the interaction between complementary, three heptad (21 amino acid) E and K peptides (E_3 and K_3). However, to achieve full fusion of liposome and cell membranes, E and K peptides must be extended to four heptad repeats (E_4/K_4, 28 amino acids) [30].

To assess the optimal PEG length necessary to sterically shield the E_4/K_4 peptide interaction, lipid mixing experiments between E_4- and K_4-liposomes were, therefore, first performed *in vitro* (**Figure 2a**). For this, photolabile cholesterol-*o*-nitrobenzyl-PEG constructs (PEG_{2000} and PEG_{5000}, see **Scheme S1** for chemical structure) were incorporated (*via* post-modification), at varying mol% (0-10 mol%) within E_4-liposome formulations (see Supporting Information for size and zeta potentials of all liposomes, **Figure S1** for TEM images of E_{PEG}- and F_{PEG}-liposomes). As photocleavable functionality, methoxy-functionalised *o*-nitrobenzyl groups were selected as: 1) they have been successfully used as photocage of a variety of bioactive compounds and biomolecules in complex biological solutions, 2) they have rapid photolysis kinetics, and 3), as the methyl substituted variant (at the benzylic position), the evolved nitroso photolytic by-products are less toxic than unsubstituted nitroso variants [36]. Now with larger,

tetrameric E_4 and K_4 peptides displayed from liposome surface, PEG_{2000} was shown ineffective at shielding the interaction between complementary peptides, as evidenced by significant lipid mixing of E- and K-liposome membranes even at high incorporated mol% of PEG. In contrast, >2 mol% cholesterol-PEG_{5000} incorporated within the E-liposome membrane was sufficient to completely shield the E4/K4 interaction. Furthermore, upon UV irradiation (15 mins, 370 ± 7 nm, 202 mW/cm^2, see **Figure S2** for dePEGylation efficiency) of an equimolar solution of K-liposomes and E_{PEG}-liposomes (4 mol% photolabile cholesterol-PEG_{5000}), complete restoration of lipid mixing of K- and E-liposome membranes (**Figure 2a**) and a concomitant increase in liposome size, due to the fusion of two or more distinct liposomes (**Figure S3**), was observed. Given the significantly smaller molecular size of folate, we assumed 4 mol% PEG_{5000} would be amply sufficient to sterically mask displayed folate functionality from the F-liposome surface. E_{PEG}-liposomes (containing 4 mol% photolabile cholesterol-PEG_{5000}) were stable in aqueous media (+ 10% serum) for at least 20h at room temperature (**Figure S4**).

Next, light induced liposome-cell interactions, mediated through E/K complexation, were assessed *in vitro* (**Figure 2b-d**). For these experiments, HeLa cells were pre-functionalised with lipopeptide K_4 constructs (to form K-functionalised cells), as previously described [37]. E_{PEG}-liposomes (400 μM, 4 mol% PEG_{2000} *or* PEG_{5000}) – containing a fluorescent lipid probe (1 mol% DOPE-NBD, green) and encapsulated propidium iodide (PI, a turn-on intercalator, 75 μM, red) – were incubated with K-functionalised cells, washed and imaged, both before and after UV irradiation (15 mins, 370 ± 7 nm, 50.6 mW/cm^2, *light dose* = 45.5 J/cm^2). Under analogous irradiation conditions and experimental setups, no photocytotoxicity was observed [24]. Supporting lipid mixing experiments, E_{PEG}-liposomes (PEG_{2000}, 4 mol%), prior to light irradiation, interacted with K-functionalised HeLa cells (**Figure 2b**), confirming PEG_{2000} is an insufficient steric shield in blocking E_4/K_4 interactions in both liposome-liposome and liposome-cell fusion experiments. In contrast, prior to light triggered dePEGylation, E_{PEG}-liposomes (PEG_{5000}, 4 mol%) showed no interaction with cells nor intracellular PI delivery (**Figure 2c**). However, subsequent *in situ* UV irradiation (15 mins, 370 ± 7 nm, 50.6 mW/cm^2, *light dose* = 45.5 J/cm^2) resulted in HeLa cell membranes homogenously labelled with liposome-associated lipid probes (DOPE-NBD) and PI clearly dispersed within the cell cytosol (**Figure 2d**). Analogous localization and homogenous dispersion of lipid probes throughout target plasma cell membranes (rather than punctae within cells, indicative of endosomal uptake) was previously observed in E_4/K_4 mediated liposome-cell fusion experiments, including in the presence of various endocytosis inhibitors [30]. From these experiments, 4 mol% PEG_{5000} displayed on the surface of E_4-liposomes was deemed sufficient to inhibit putative E_4/K_4 mediated liposome-cell fusion and, by using photolabile lipid-PEG constructs, precise spatiotemporal control over liposome-cell membrane fusion could be achieved (**Figure S5**).

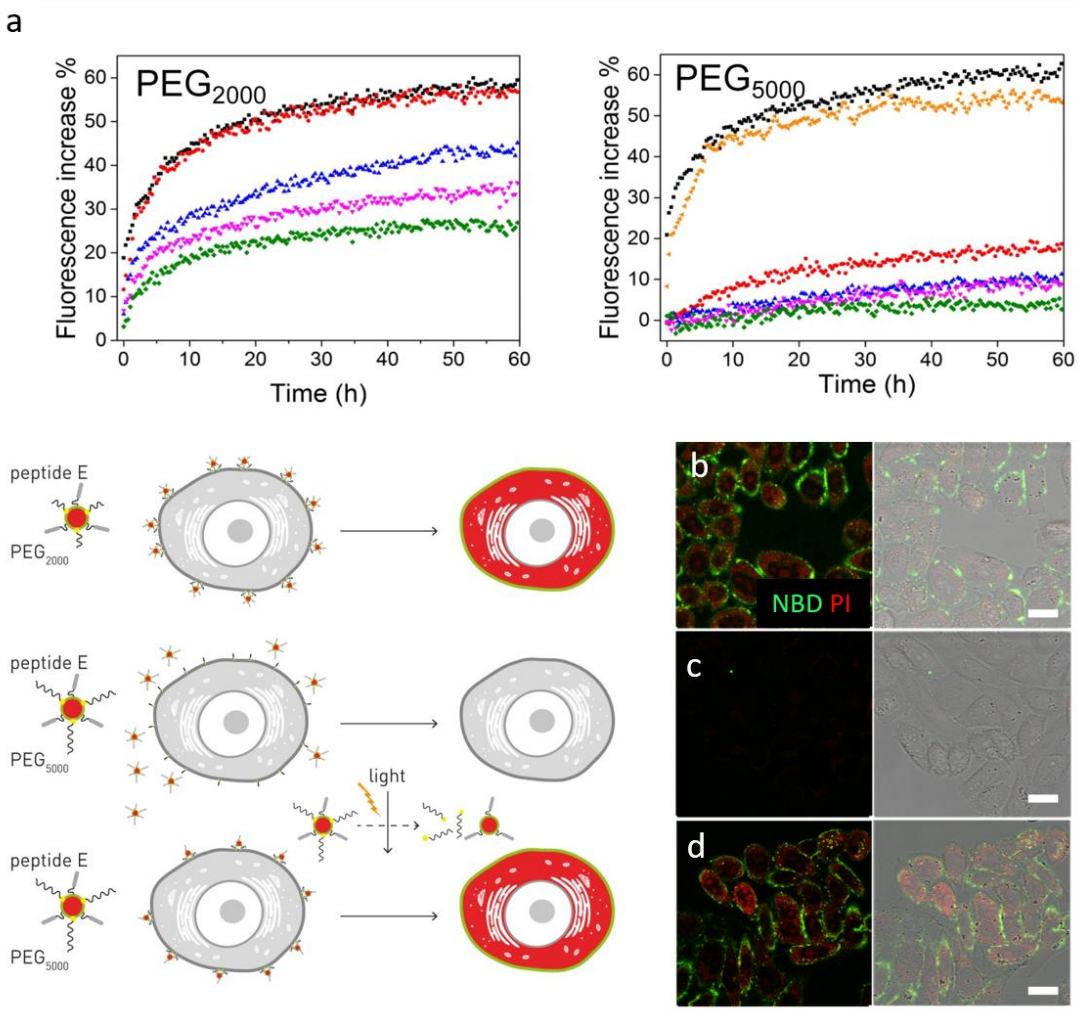

Figure 2 Optimisation of required PEG length. A. Lipid mixing experiments of E- and K-liposomes incorporating varying mol% cholesterol-nitrobenzyl-PEG_{2000} (left) or cholesterol-nitrobenzyl-PEG_{5000} (right) within E-liposome formulations. 0 mol% (black), 2 mol% (red), 4 mol% (blue), 8 mol% (pink) and 10 mol% (green), 4mol% following UV irradiation (15min, 370 ± 7 nm, 202 mW/cm^2) (orange). Liposome-cell fusion of E_{PEG}-liposomes (4 mol% PEG_{2000}, – before UV, (**B**); 4 mol% PEG_{5000} before (**C**) and after (**D**) applied UV light (15 mins, 370 ± 7 nm, 50.6 mW/cm^2, *light dose* = 45.5 J/cm^2). E_{PEG}-liposomes contained 1 mol% DOPE-NBD (lipid probe, green) and encapsulated PI (75 µM, turn-on intercalator, red), scale bars = 30 µm.

Next, light triggered, active targeting of liposomes to xenograft MDA-MB-231 breast cancer cells was assessed within live embryonic zebrafish (**Figure 3**). Both F-liposomes, targeting the overexpressed folate receptor on MDA-MB-231 cells [28,29], and E-liposomes, targeting K-functionalised MDA-MB-231 cells, were independently tested. Zebrafish embryos are small (2-3 mm in length) and transparent enabling fluorescence imaging of specific biological events across entire living organisms in real time [38]. Zebrafish are increasingly used as model organisms to study fundamental processes such as embryogenesis, cell migration, sleep and disease pathogenesis [39,40]. This includes the development of embryonic zebrafish xenograft models to study the pathogenesis of human cancers [41-43], including human breast cancers [44,45]. Here, MDA-MB-231 breast cancer cells, stably expressing GFP, were

microinjected into the circulation of 2-day old zebrafish larvae *via* the duct of Cuvier and quickly accumulated (<1 hours post injection (hpi)) within the caudal hematopoietic tissue (CHT) [46]. One hour after injection of cancer cells, either fluorescently labelled E_{PEG}- or F_{PEG}-liposomes (4 mol% PEG_{5000}, 1 mol% DOPE-LR probe) were injected (1 mM, 3 nL) into circulation *via* the posterior cardinal vein (PCV). Prior to UV irradiation, both E_{PEG}- and F_{PEG}-liposomes freely circulated, were confined within the vasculature of the embryo, and no co-localization of liposomes with either xenograft cancer cells or key RES cell types of the embryonic zebrafish (*e.g.* scavenging endothelial cells (SECs) or blood resident macrophages) [47], was observed (**Figure 3**).

Following *in situ* UV irradiation (15 mins, 370 ± 7 nm, 13.5 mW/cm^2, *light dose* = 0.45 J/embryo) of the embryonic fish, however, both E- and F-liposomes rapidly and selectively co-localised with xenograft cancer cells (<30 min, i.e. prior to first image acquisition) (**Figure 3**). Under these irradiation conditions, embryos continued to develop normally (up to 6 days post-fertilisation (dpf)) and no phenotypic abnormalities were observed (**Figure S6**). Under identical conditions, the biodistribution of F_{PEG}-liposomes containing non-cleavable PEG_{5000} (DSPE-PEG_{5000}, Avanti) remained unchanged before and after *in situ* light irradiation, demonstrating the targeting requirement of both liposomes containing photocleavable PEG as well as UV light (**Figure S7**). In the case of E-liposomes, E/K specificity was confirmed by repeating the experiment in the absence of peptide K (displayed from xenografted cancer cells). In this case, no E-liposome accumulation with cancer cells was observed following UV irradiation, confirming the requirement and selectivity of E_4/K_4 recognition and complexation for cell specific targeting (**Figure S8**).

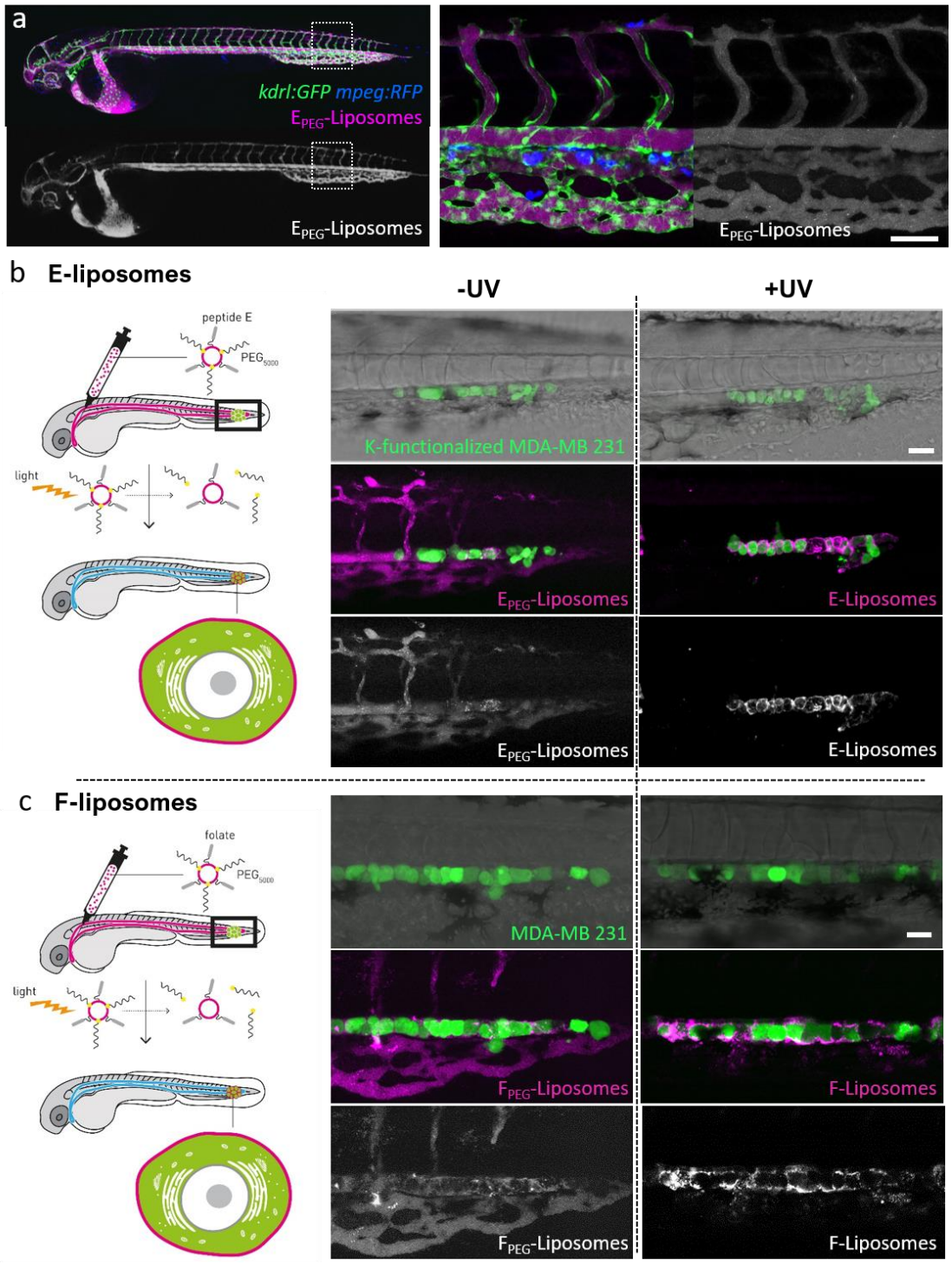

Figure 3 Cancer cell-specific, light triggered liposome-cell interactions *in vivo*. A. Biodistribution of E_{PEG}-liposomes (1 mM, 4 mol% PEG_{5000}, containing 1 mol% DOPE-Atto 633, far red) in *Tg(kdrl:GFP/mpeg:RFP)* zebrafish embryos (2 dpf), following i.v. injection. Liposomes are confined within the vasculature of the embryo and freely circulate. No liposome co-localisation with either endothelial cells (green) or (blood resident) macrophages (blue) is observed indicative of the ability of E_{PEG}-liposomes to evade key RES cell types. Confocal z-stacks acquired at 1hpi. **B,C.** MDA-MB-231 human breast cancer cells, stably expressing GFP, were injected into the circulation of a 2-day old zebrafish embryo and quickly accumulated in the caudal hematopoietic tissue (CHT). In the case of E-liposomes, cells were pre-treated with lipopetide K. Into this xenograft model, either E_{PEG}- or F_{PEG}-liposomes (1 mM, 4 mol% PEG_{5000},

containing 1 mol% DOPE-LR, red) were injected into circulation. Prior to UV irradiation, both E_{PEG}- or F_{PEG}-liposomes were freely circulating, confined within the vasculature of the fish (left image panels). Following UV irradiation (15 mins, 370 ± 7 nm, 13.5 mW/cm^2, *light dose* = 0.45 J/embryo) and photolytic dePEGylation, both E- and F-liposomes selectively bound to xenograft cancer cells within the CHT (right image panels). Data are representative of three independent experiments (each n=5). Field of view = boxed region in embryo cartoon. Scale bars = 100 µm.

Extending our approach to liposome mediated, intracellular drug delivery, we first measured the *in vitro* cytotoxicity (MDA-MB 231 cells, WST assay) of doxorubicin-filled E_{PEG}- and F_{PEG}-liposomes (4 mol% PEG_{5000}), before and after light activation, and compared this to the toxicity of free doxorubicin (**Figure 4a**). Again, for experiments involving E_{PEG}-liposomes, cells were first pretreated with lipopeptide K. For both E_{PEG}- and F_{PEG}-liposomes, cell viability was unaffected in the absence of applied UV light, and, in the case of E_{PEG}-liposomes, no intracellular DOX delivery was observed (**Figure 4b**, F_{PEG}-liposomes were not analyzed under the fluorescence microscope). Upon light triggered dePEGylation, however, both E- and F-liposome mediated delivery of doxorubicin led to enhanced cytotoxicity (IC_{50} approx. 100 µM and 200 µM, respectively for E- and F-lipo-DOX) compared to free DOX (IC_{50} approx. 300 µM). Interestingly, under these experimental conditions, the most potent cytotoxicity was observed for E/K mediated liposomal delivery of DOX. This suggests DOX delivery direct to the cell cytosol, following liposome-cell membrane fusion, is a potentially potent method of drug delivery. Importantly, freshly prepared DOX-loaded liposomes used in all cases, as significant DOX leakage (30-40%) from the liposome core was observed for all formulations during prolonged storage and would affect the efficiency of liposomal DOX delivery over time (**Figure S9**).

Next, doxorubicin-filled E_{PEG}-liposomes (4 mol% PEG_{5000}, 250 µM doxorubicin) were intravenously microinjected into embryonic zebrafish xenografts (K-functionalised MDA-MB-231 breast cancer cells) (**Figure 4c)** and the efficacy in reducing tumor burdens assessed (**Figure 4d and 4e**). For this, relative cancer cell proliferation was quantified by measuring total GFP fluorescence of xenograft cancer cells. Here, significantly ($p<0.0001$) reduced cancer cell proliferation (46.9% reduction) was only observed in the '+UV' group. In the absence of light, tumor proliferation was unaffected and no significant difference in cancer cell numbers was measured compared to the untreated controls. Again, using cancer cells unfunctionalized with peptide K, no reduction in cancer cell proliferation was observed (**Figure S10**), further emphasising the essential requirement and selectivity of E_4/K_4 recognition and complexation.

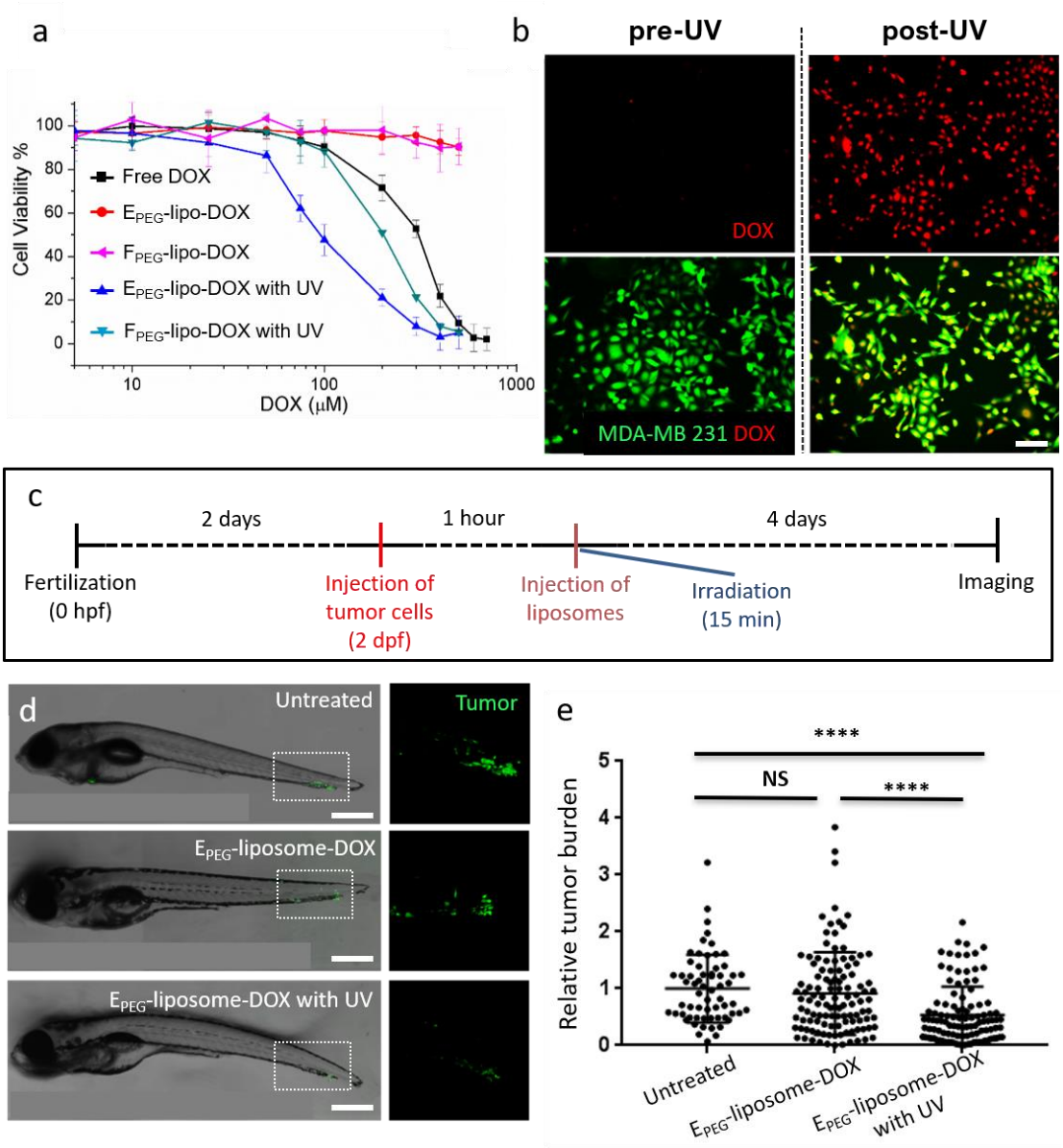

Figure 4 Delivery of liposome-encapsulated doxorubicin to MDA-MB 231 cells both *in vitro* and *in vivo*. a. MDA-MB-231 breast cancer cell viability *in vitro* (measured by WST assay) following 2 h incubation with either DOX-filled E_{PEG}-liposomes (4 mol% PEG_{5000}), before (red) and after (blue) UV activation (15 mins, 370 ± 7 nm, 50.6 mW/cm^2, *light dose* = 45.5 J/cm^2); F_{PEG}-liposomes (4 mol% PEG_{5000}), before (pink) and after (cyan) UV activation; or free doxorubicin (black) without UV irradiation. For +UV samples, liposomes were added to cells and immediately irradiated. 2 h incubation time includes 15 min irradiation time. In the absence of light, both E_{PEG}- and F_{PEG}-lipo-DOX formulations were non-toxic. Following light activation, liposome mediated delivery of doxorubicin resulted in enhanced cytotoxicity (F-liposomes, IC_{50} = approx. 200 μM; E-liposomes, IC_{50} = approx. 100 μM) compared to free doxorubicin (IC_{50} = approx. 300 μM). In all cases, freshly prepared DOX-filled liposomes were used to minimize the effects of DOX leakage over time. **b**. Intracellular DOX delivery by E_{PEG}-liposomes (200 μM encapsulated DOX, red) and K-functionalised MDA-MB-231 breast cancer cells, stably expressing GFP, green, before (left) and after (right) UV irradiation (15 mins, 370 ± 7 nm, 50.6 mW/cm^2, *light dose* = 45.5 J/cm^2). Scale bars=100 μm. **c.** Timeline of zebrafish development, MDA-MB-231 cell injection, liposome injection and quantification in the zebrafish embryo. At 2 dpf, MDA-MB-231 cells (approx. 300 cells) were injected into circulation *via* the duct of Cuvier. One hour after

engraftment, DOX-filled, E_{PEG}-liposomes (3nl, 4mM total lipid; 200 µM encapsulated doxorubicin) were injected into circulation *via* the posterior cardinal vein. UV irradiation (15 mins, 370 ± 7 nm, 13.5 mW/cm^2, *light dose* = 0.45 J/embryo), where appropriate, was performed immediately after the injection of liposomes. Tumor burden analysed at 4 dpi. **d,e**. Visualisation and quantification of cancer proliferation in the zebrafish embryo. Significant ($P<0.0001$) reduction in tumor volume was only observed for DOX-filled, E_{PEG}-liposomes, following in situ light activation. In the absence of light activation, tumor progression/burden was unaffected as for untreated controls. Data is presented as mean values ± SD, each point on the scatter plots represents one larva. Brackets indicate significantly different values (****, $p < 0.0001$; NS, not significant) based on one-way ANOVA statistical testing. n = 61 individually injected embryos (untreated group). n = 114 (without UV group) and n = 108 (with UV group). Scale bars = 500 µm.

Conclusion

Here, we successfully demonstrate light triggered targeting of liposomes to xenograft cancer cells *in vivo*. Our approach relies on the light triggered dePEGylation of liposome surfaces, revealing underlying targeting functionality. General applicability of this approach was demonstrated using both an experimental two component fusion system (peptides E and K) as well as clinically relevant folate-decorated liposomes. Both E_{PEG}- and F_{PEG}-liposomes, prior to light triggered activation, freely circulated throughout the vasculature of the embryonic zebrafish, and showed no significant interactions with either target cancer cells or key RES cell types (scavenging endothelial cells or blood resident macrophages) within the fish [47]. In mammals, analogous RES cell types, namely liver sinusoidal endothelial cells (LSECs), Kupffer cells (hepatic, blood resident macrophages) and splenic macrophages, are responsible for the clearance of the majority of *i.v.* administered nanoparticles from the body [48]. While there is currently no established model for the EPR effect in embryonic zebrafish, the implications of our findings are that both E_{PEG}- and clinically relevant F_{PEG}-liposomes, prior to light activation, would likely evade RES clearance in mammals, prolonging circulation lifetimes and the potential for liposome accumulation in pathological tissues with enhanced permeability.

In the case of E-liposome targeting, prior modification of cancer cell membranes with complementary peptide K is a pre-requisite. While this system provides us with a fundamental tool to probe alternative liposomal drug delivery routes (*i.e.* fusion vs. endocytosis), as well as a highly selective handle for targeting as is shown in this study, the necessity for components displayed from both liposome and target cell membranes is a major limitation to further *in vivo* application. Similarly, the use of UV light as a trigger raises valid concerns over applicability in larger, non-transparent mammals, including humans. To some extent, these concerns relate to the poor tissue penetration of UV light (approx. 100-200 µm). As a result, the clinical use of UV light is restricted to the topical treatment of cosmetic skin disorders, including psoriasis, acne and eczema [49]. However, these limitations are increasingly being overcome, as fundamental advances in fiber optic [18] and wireless LED technologies [19,20] facilitate the localized delivery of UV light deep within patients. Alternatively, extended exposure to UV light is known to pose a significant health risk, with the potential to cause DNA damage, cytotoxicity and cancer

[50]. In this study, applied UV-A (370 ± 7 nm) light doses to zebrafish embryos (12.1 J/cm^2) are well below recommended (skin) exposure limits (32 J/cm^2 @ 375 nm). Furthermore, while single photon UV-A (370 nm) light is optimal for the photolysis of *o*-nitrobenzyl functionalities, the use of 2-photon excitation sources [51,52] or photolabile chemistries sensitive to longer wavelength, visible light [53,54], offer options for light activation both deep in tissue and with reduced photocytotoxicity.

Finally, this study highlights the unique opportunities offered by the embryonic zebrafish model in the design and optimization of nanomedicines. In this study, we were able to 1) generate our desired xenograft cancer model without the need for immunosuppression (the adaptive immune system is not yet developed zebrafish embryos), 2) directly visualize the changing pharmacokinetics of stimuli-responsive nanoparticles *in situ*, *in vivo* and in real time and 3) set-up and perform efficacy studies, involving several hundred animals, within 1 week. The combined level of detailed assessment, low cost and experimental speed, afforded by the embryonic zebrafish model, is simply not achievable using conventional animal models (eg. mice and rats). As to the predictive potential of the embryonic zebrafish, we, and others, have recently shown both pharmacokinetic parameters and key cellular interactions of nanomedicines are highly conserved between the embryonic zebrafish and mice [47,55].

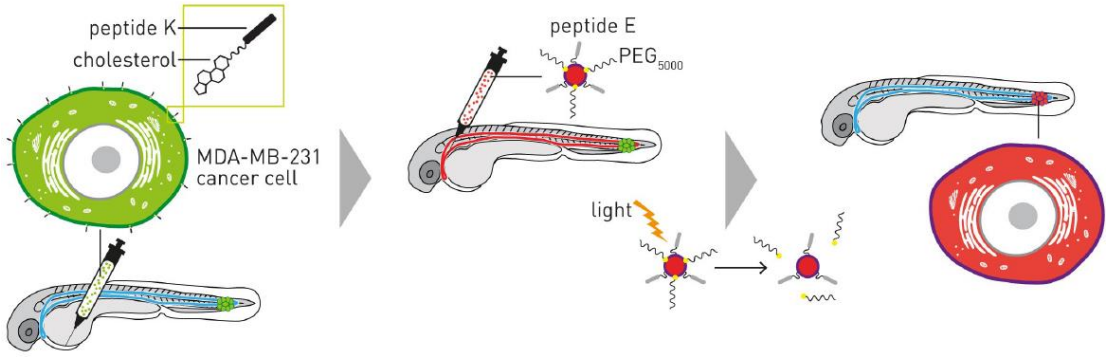

Cancer cell-specific drug delivery remains a major unmet challenge for nanomedicines. In this work, we use light to 'turn on' the targeting of nanomedicines, *in situ* and *in vivo*, enabling on demand cancer cell specific drug delivery in live zebrafish embryos.

Acknowledgements This work was funded through Chinese Scholarship Council grants (LK,QC) and the Netherlands Organization for Scientific Research (NWO-Vici-project nr. 724.014.001; FC, AK). Arwin Groenewoud (Institute of Biology, Leiden University) is thanked for the kind gift of Plasmid #106172 (Addgene.org). Infographics were developed by Joost Bakker (www.scicomvisuals.com).

References

1. Ventola, C.L. Progress in Nanomedicine: Approved and Investigational Nanodrugs. *P & T : a peer-reviewed journal for formulary management* **2017**, *42*, 742-755.
2. Shi, J.; Kantoff, P.W.; Wooster, R.; Farokhzad, O.C. Cancer nanomedicine: progress,

challenges and opportunities. *Nat Rev Cancer* **2017**, *17*, 20-37, doi:10.1038/nrc.2016.108.
3. Maeda, H.; Wu, J.; Sawa, T.; Matsumura, Y.; Hori, K. Tumor vascular permeability and the EPR effect in macromolecular therapeutics: a review. *Journal of controlled release : official journal of the Controlled Release Society* **2000**, *65*, 271-284, doi:10.1016/s0168-3659(99)00248-5.
4. Maeda, H.; Nakamura, H.; Fang, J. The EPR effect for macromolecular drug delivery to solid tumors: Improvement of tumor uptake, lowering of systemic toxicity, and distinct tumor imaging in vivo. *Advanced drug delivery reviews* **2013**, *65*, 71-79, doi:10.1016/j.addr.2012.10.002.
5. Immordino, M.L.; Dosio, F.; Cattel, L. Stealth liposomes: review of the basic science, rationale, and clinical applications, existing and potential. *International journal of nanomedicine* **2006**, *1*, 297-315.
6. Suk, J.S.; Xu, Q.; Kim, N.; Hanes, J.; Ensign, L.M. PEGylation as a strategy for improving nanoparticle-based drug and gene delivery. *Advanced drug delivery reviews* **2016**, *99*, 28-51, doi:10.1016/j.addr.2015.09.012.
7. Fritze, A.; Hens, F.; Kimpfler, A.; Schubert, R.; Peschka-Süss, R. Remote loading of doxorubicin into liposomes driven by a transmembrane phosphate gradient. *Biochimica et biophysica acta* **2006**, *1758*, 1633-1640, doi:10.1016/j.bbamem.2006.05.028.
8. Byrne, J.D.; Betancourt, T.; Brannon-Peppas, L. Active targeting schemes for nanoparticle systems in cancer therapeutics. *Advanced drug delivery reviews* **2008**, *60*, 1615-1626, doi:10.1016/j.addr.2008.08.005.
9. Bazak, R.; Houri, M.; El Achy, S.; Kamel, S.; Refaat, T. Cancer active targeting by nanoparticles: a comprehensive review of literature. *Journal of cancer research and clinical oncology* **2015**, *141*, 769-784, doi:10.1007/s00432-014-1767-3.
10. Mishra, S.; Webster, P.; Davis, M.E. PEGylation significantly affects cellular uptake and intracellular trafficking of non-viral gene delivery particles. *European journal of cell biology* **2004**, *83*, 97-111, doi:10.1078/0171-9335-00363.
11. Fang, Y.; Xue, J.; Gao, S.; Lu, A.; Yang, D.; Jiang, H.; He, Y.; Shi, K. Cleavable PEGylation: a strategy for overcoming the "PEG dilemma" in efficient drug delivery. *Drug delivery* **2017**, *24*, 22-32, doi:10.1080/10717544.2017.1388451.
12. Kong, L.; Campbell, F.; Kros, A. DePEGylation strategies to increase cancer nanomedicine efficacy. *Nanoscale horizons* **2019**, *4*, 378-387, doi:10.1039/c8nh00417j.
13. Webb, B.A.; Chimenti, M.; Jacobson, M.P.; Barber, D.L. Dysregulated pH: a perfect storm for cancer progression. *Nat Rev Cancer* **2011**, *11*, 671-677, doi:10.1038/nrc3110.
14. Mehner, C.; Hockla, A.; Miller, E.; Ran, S.; Radisky, D.C.; Radisky, E.S. Tumor cell-produced matrix metalloproteinase 9 (MMP-9) drives malignant progression and metastasis of basal-like triple negative breast cancer. *Oncotarget* **2014**, *5*, 2736-2749, doi:10.18632/oncotarget.1932.
15. Vaupel, P.; Kallinowski, F.; Okunieff, P. Blood flow, oxygen and nutrient supply, and metabolic microenvironment of human tumors: a review. *Cancer Res* **1989**, *49*, 6449-6465.
16. Karotki, A.; Khurana, M.; Lepock, J.R.; Wilson, B.C. Simultaneous two-photon excitation of photofrin in relation to photodynamic therapy. *Photochemistry and photobiology* **2006**, *82*, 443-452, doi:10.1562/2005-08-24-ra-657.
17. Bolze, F.; Jenni, S.; Sour, A.; Heitz, V. Molecular photosensitisers for two-photon photodynamic therapy. *Chem Commun (Camb)* **2017**, *53*, 12857-12877, doi:10.1039/c7cc06133a.
18. Yun, S.H.; Kwok, S.J.J. Light in diagnosis, therapy and surgery. *Nature biomedical engineering* **2017**, *1*, doi:10.1038/s41551-016-0008.
19. Kim, T.I.; McCall, J.G.; Jung, Y.H.; Huang, X.; Siuda, E.R.; Li, Y.; Song, J.; Song, Y.M.; Pao, H.A.; Kim, R.H., et al. Injectable, cellular-scale optoelectronics with applications for wireless optogenetics. *Science (New York, N.Y.)* **2013**, *340*, 211-216, doi:10.1126/science.1232437.
20. Bansal, A.; Yang, F.; Xi, T.; Zhang, Y.; Ho, J.S. In vivo wireless photonic photodynamic therapy. *Proceedings of the National Academy of Sciences of the United States of America* **2018**, *115*, 1469-1474, doi:10.1073/pnas.1717552115.
21. Wang, J.; Ouyang, Y.; Li, S.; Wang, X.; He, Y. Photocleavable amphiphilic diblock copolymer with an azobenzene linkage. *RSC Advances* **2016**, *6*, 57227-57231, doi:10.1039/C6RA12129B.

22. Saravanakumar, G.; Park, H.; Kim, J.; Park, D.; Pramanick, S.; Kim, D.H.; Kim, W.J. Miktoarm Amphiphilic Block Copolymer with Singlet Oxygen-Labile Stereospecific β-Aminoacrylate Junction: Synthesis, Self-Assembly, and Photodynamically Triggered Drug Release. *Biomacromolecules* **2018**, *19*, 2202-2213, doi:10.1021/acs.biomac.8b00290.
23. Jin, Q.; Cai, T.; Han, H.; Wang, H.; Wang, Y.; Ji, J. Light and pH dual-degradable triblock copolymer micelles for controlled intracellular drug release. *Macromolecular rapid communications* **2014**, *35*, 1372-1378, doi:10.1002/marc.201400171.
24. Kong, L.; Poulcharidis, D.; Schneider, G.F.; Campbell, F.; Kros, A. Spatiotemporal Control of Doxorubicin Delivery from "Stealth-Like" Prodrug Micelles. *International journal of molecular sciences* **2017**, *18*, doi:10.3390/ijms18102033.
25. Zhou, D.; Guo, J.; Kim, G.B.; Li, J.; Chen, X.; Yang, J.; Huang, Y. Simultaneously Photo-Cleavable and Activatable Prodrug-Backboned Block Copolymer Micelles for Precise Anticancer Drug Delivery. *Advanced healthcare materials* **2016**, *5*, 2493-2499, doi:10.1002/adhm.201600470.
26. Kalva, N.; Parekh, N.; Ambade, A.V. Controlled micellar disassembly of photo- and pH-cleavable linear-dendritic block copolymers. *Polymer Chemistry* **2015**, *6*, 6826-6835, doi:10.1039/C5PY00792E.
27. Zhou, M.; Huang, H.; Wang, D.; Lu, H.; Chen, J.; Chai, Z.; Yao, S.Q.; Hu, Y. Light-Triggered PEGylation/dePEGylation of the Nanocarriers for Enhanced Tumor Penetration. *Nano letters* **2019**, *19*, 3671-3675, doi:10.1021/acs.nanolett.9b00737.
28. Hartmann, L.C.; Keeney, G.L.; Lingle, W.L.; Christianson, T.J.; Varghese, B.; Hillman, D.; Oberg, A.L.; Low, P.S. Folate receptor overexpression is associated with poor outcome in breast cancer. *International journal of cancer* **2007**, *121*, 938-942, doi:10.1002/ijc.22811.
29. Meier, R.; Henning, T.D.; Boddington, S.; Tavri, S.; Arora, S.; Piontek, G.; Rudelius, M.; Corot, C.; Daldrup-Link, H.E. Breast cancers: MR imaging of folate-receptor expression with the folate-specific nanoparticle P1133. *Radiology* **2010**, *255*, 527-535, doi:10.1148/radiol.10090050.
30. Yang, J.; Bahreman, A.; Daudey, G.; Bussmann, J.; Olsthoorn, R.C.; Kros, A. Drug Delivery via Cell Membrane Fusion Using Lipopeptide Modified Liposomes. *ACS central science* **2016**, *2*, 621-630, doi:10.1021/acscentsci.6b00172.
31. Robson Marsden, H.; Elbers, N.A.; Bomans, P.H.; Sommerdijk, N.A.; Kros, A. A reduced SNARE model for membrane fusion. *Angewandte Chemie (International ed. in English)* **2009**, *48*, 2330-2333, doi:10.1002/anie.200804493.
32. Kong, L.; Askes, S.H.; Bonnet, S.; Kros, A.; Campbell, F. Temporal Control of Membrane Fusion through Photolabile PEGylation of Liposome Membranes. *Angewandte Chemie (International ed. in English)* **2016**, *55*, 1396-1400, doi:10.1002/anie.201509673.
33. Ellett, F.; Pase, L.; Hayman, J.W.; Andrianopoulos, A.; Lieschke, G.J. mpeg1 promoter transgenes direct macrophage-lineage expression in zebrafish. *Blood* **2011**, *117*, e49-56, doi:10.1182/blood-2010-10-314120.
34. Schindelin, J.; Arganda-Carreras, I.; Frise, E.; Kaynig, V.; Longair, M.; Pietzsch, T.; Preibisch, S.; Rueden, C.; Saalfeld, S.; Schmid, B., et al. Fiji: an open-source platform for biological-image analysis. *Nature methods* **2012**, *9*, 676-682, doi:10.1038/nmeth.2019.
35. Tomatsu, I.; Marsden, H.R.; Rabe, M.; Versluis, F.; Zheng, T.; Zope, H.; Kros, A. Influence of pegylation on peptide-mediated liposome fusion. *Journal of Materials Chemistry* **2011**, *21*, 18927-18933, doi:10.1039/C1JM11722J.
36. Klán, P.; Šolomek, T.; Bochet, C.G.; Blanc, A.; Givens, R.; Rubina, M.; Popik, V.; Kostikov, A.; Wirz, J. Photoremovable protecting groups in chemistry and biology: reaction mechanisms and efficacy. *Chemical reviews* **2013**, *113*, 119-191, doi:10.1021/cr300177k.
37. Zope, H.R.; Versluis, F.; Ordas, A.; Voskuhl, J.; Spaink, H.P.; Kros, A. In vitro and in vivo supramolecular modification of biomembranes using a lipidated coiled-coil motif. *Angewandte Chemie (International ed. in English)* **2013**, *52*, 14247-14251, doi:10.1002/anie.201306033.
38. Sieber, S.; Grossen, P.; Bussmann, J.; Campbell, F.; Kros, A.; Witzigmann, D.; Huwyler, J. Zebrafish as a preclinical in vivo screening model for nanomedicines. *Advanced drug delivery reviews* **2019**, *151-152*, 152-168, doi:10.1016/j.addr.2019.01.001.
39. Santoriello, C.; Zon, L.I. Hooked! Modeling human disease in zebrafish. *The Journal of clinical investigation* **2012**, *122*, 2337-2343, doi:10.1172/jci60434.

40. Cronan, M.R.; Tobin, D.M. Fit for consumption: zebrafish as a model for tuberculosis. *Disease models & mechanisms* **2014**, *7*, 777-784, doi:10.1242/dmm.016089.
41. Grabher, C.; Look, A.T. Fishing for cancer models. *Nature biotechnology* **2006**, *24*, 45-46, doi:10.1038/nbt0106-45.
42. Konantz, M.; Balci, T.B.; Hartwig, U.F.; Dellaire, G.; André, M.C.; Berman, J.N.; Lengerke, C. Zebrafish xenografts as a tool for in vivo studies on human cancer. *Annals of the New York Academy of Sciences* **2012**, *1266*, 124-137, doi:10.1111/j.1749-6632.2012.06575.x.
43. Drabsch, Y.; Snaar-Jagalska, B.E.; Ten Dijke, P. Fish tales: The use of zebrafish xenograft human cancer cell models. *Histology and histopathology* **2017**, *32*, 673-686, doi:10.14670/hh-11-853.
44. Tulotta, C.; Stefanescu, C.; Beletkaia, E.; Bussmann, J.; Tarbashevich, K.; Schmidt, T.; Snaar-Jagalska, B.E. Inhibition of signaling between human CXCR4 and zebrafish ligands by the small molecule IT1t impairs the formation of triple-negative breast cancer early metastases in a zebrafish xenograft model. *Disease models & mechanisms* **2016**, *9*, 141-153, doi:10.1242/dmm.023275.
45. Drabsch, Y.; He, S.; Zhang, L.; Snaar-Jagalska, B.E.; ten Dijke, P. Transforming growth factor-β signalling controls human breast cancer metastasis in a zebrafish xenograft model. *Breast Cancer Res* **2013**, *15*, R106, doi:10.1186/bcr3573.
46. de Boeck, M.; Cui, C.; Mulder, A.A.; Jost, C.R.; Ikeno, S.; Ten Dijke, P. Smad6 determines BMP-regulated invasive behaviour of breast cancer cells in a zebrafish xenograft model. *Scientific reports* **2016**, *6*, 24968, doi:10.1038/srep24968.
47. Campbell, F.; Bos, F.L.; Sieber, S.; Arias-Alpizar, G.; Koch, B.E.; Huwyler, J.; Kros, A.; Bussmann, J. Directing Nanoparticle Biodistribution through Evasion and Exploitation of Stab2-Dependent Nanoparticle Uptake. *ACS nano* **2018**, *12*, 2138-2150, doi:10.1021/acsnano.7b06995.
48. Zhang, Y.N.; Poon, W.; Tavares, A.J.; McGilvray, I.D.; Chan, W.C.W. Nanoparticle-liver interactions: Cellular uptake and hepatobiliary elimination. *Journal of controlled release : official journal of the Controlled Release Society* **2016**, *240*, 332-348, doi:10.1016/j.jconrel.2016.01.020.
49. Vangipuram, R.; Feldman, S.R. Ultraviolet phototherapy for cutaneous diseases: a concise review. *Oral diseases* **2016**, *22*, 253-259, doi:10.1111/odi.12366.
50. Narayanan, D.L.; Saladi, R.N.; Fox, J.L. Ultraviolet radiation and skin cancer. *International journal of dermatology* **2010**, *49*, 978-986, doi:10.1111/j.1365-4632.2010.04474.x.
51. Furuta, T.; Wang, S.S.; Dantzker, J.L.; Dore, T.M.; Bybee, W.J.; Callaway, E.M.; Denk, W.; Tsien, R.Y. Brominated 7-hydroxycoumarin-4-ylmethyls: photolabile protecting groups with biologically useful cross-sections for two photon photolysis. *Proceedings of the National Academy of Sciences of the United States of America* **1999**, *96*, 1193-1200, doi:10.1073/pnas.96.4.1193.
52. Peng, K.; Tomatsu, I.; Korobko, A.V.; Kros, A. Cyclodextrin–dextran based in situ hydrogel formation: a carrier for hydrophobic drugs. *Soft Matter* **2010**, *6*, 85-87, doi:10.1039/B914166A.
53. Shanmugam, V.; Selvakumar, S.; Yeh, C.S. Near-infrared light-responsive nanomaterials in cancer therapeutics. *Chemical Society reviews* **2014**, *43*, 6254-6287, doi:10.1039/c4cs00011k.
54. Aujard, I.; Benbrahim, C.; Gouget, M.; Ruel, O.; Baudin, J.B.; Neveu, P.; Jullien, L. o-nitrobenzyl photolabile protecting groups with red-shifted absorption: syntheses and uncaging cross-sections for one- and two-photon excitation. *Chemistry* **2006**, *12*, 6865-6879, doi:10.1002/chem.200501393.
55. Sieber, S.; Grossen, P.; Detampel, P.; Siegfried, S.; Witzigmann, D.; Huwyler, J. Zebrafish as an early stage screening tool to study the systemic circulation of nanoparticulate drug delivery systems in vivo. *Journal of controlled release : official journal of the Controlled Release Society* **2017**, *264*, 180-191, doi:10.1016/j.jconrel.2017.08.023.

Supporting information for

Light triggered, cancer cell-specific targeting and liposomal drug delivery in a zebrafish xenograft model

Li Kong[1]⊥, Quanchi Chen[2]⊥, Frederick Campbell[1], Ewa Snaar-Jagalska[2]* and Alexander Kros[1]*

[1]Supramolecular and Biomaterials Chemistry, Leiden Institute of Chemistry, Leiden University, Einsteinweg 55, 2333 CC Leiden, The Netherlands
[2]Institute of Biology, Leiden University, Leiden 2311 EZ, The Netherlands
E-mail: a.kros@chem.leidenuniv.nl; b.e.snaar-jagalska@biology.leidenuniv.nl

a.

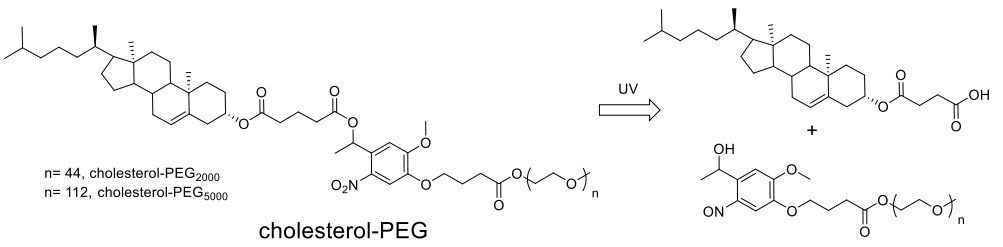

b.

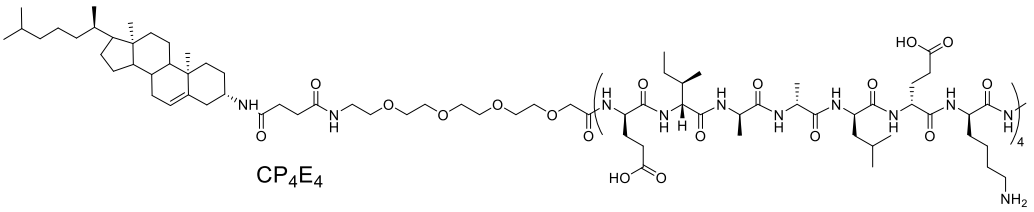

c.

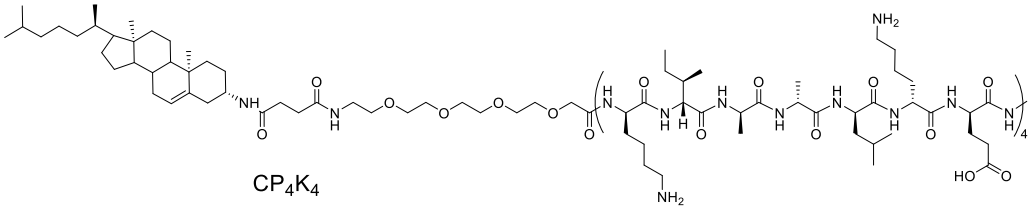

Scheme S1a. Chemical structures of cholesterol-PEG and photolysis products, **b.** Chemical structure of lipopeptide-E (CP_4E_4), **c.** Chemical structure of lipopeptide-K (CP_4K_4).

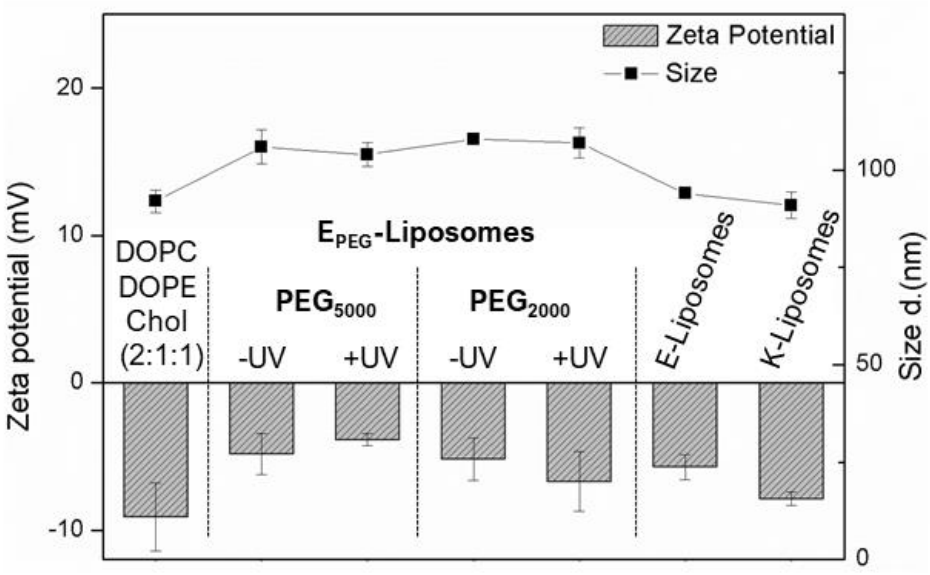

Table S1 Size and zeta potentials of E/K liposomes (containing 1mol% E or K lipopeptide). E_{PEG}-liposomes contain 4 mol% cholesterol-*o*-nitrobenzyl-PEG. Base liposome formulation (DOPC:DOPE:Chol; 2:1:1) contains neither lipopetide or PEG. No significant differences in size were observed for E_{PEG}-liposomes containing 2, 6, 8 or 10mol% PEG (data not shown). Light irradiation (15 mins, 370 ± 7 nm, 202 mW/cm^2)

F_{PEG}-liposomes (1mol% DPPE-Folate, 4mol% PEG_{5000})	**Size d. (nm)**	**PDI**	**Zeta potential (mV)**
-UV	91.3	0.10	-7.9
+UV	92.1	0.13	-6.2

Table S2 Size and zeta potentials of F_{PEG}-liposomes before and after light irradiation (15 mins, 370 ± 7 nm, 202 mW/cm^2)

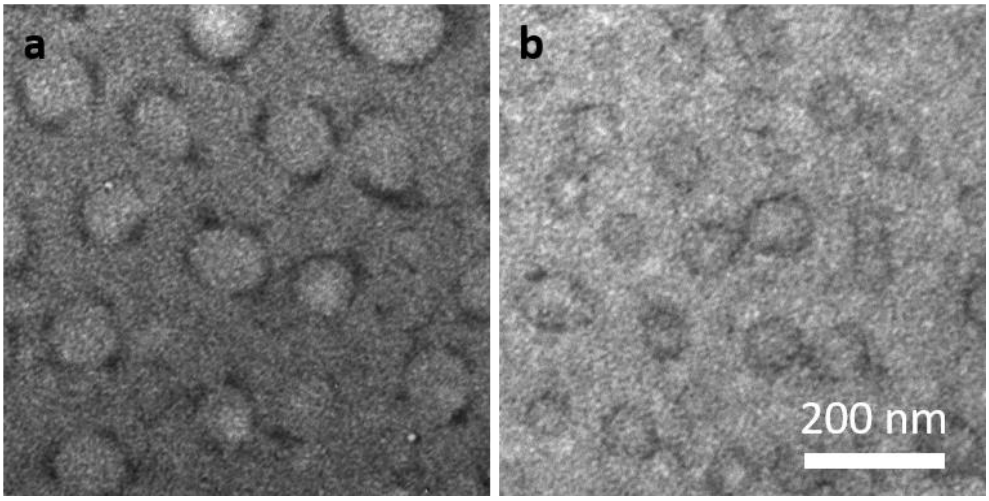

Figure S1 TEM images (TPA stained) of E_{PEG}-liposomes (a) and F_{PEG}-liposomes (b) (total lipid =1 mM, 4 mol% PEG_{5000}, 1 mol% lipopeptide E_4 or DPPE-Folate). Average size of E_{PEG}-liposomes and F_{PEG}-liposomes is 98 nm and 82 nm respectively.

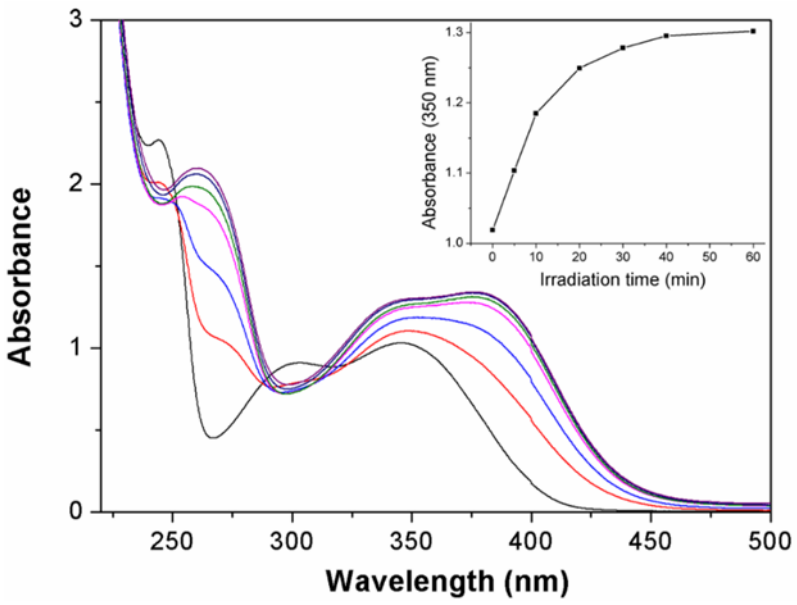

Figure S2 UV-Vis spectra of the photolysis of a solution of E_{PEG}-Liposomes (total lipid = 5 mM, 4 mol% PEG_{5000}, 1 mol% lipopeptide E_4). *Inset*: Reaction profile over time as a function of UV absorption at 350 nm. Irradiation times: 0 (black), 5 (red), 10 (blue), 20 (pink), 30 (green), 40 (navy) and 60 min (violet). The isobestic points appeared at 250 nm, 287 nm and 322 nm.

Note: UV light source used for this experiment was less intense than the LED used in all other experiments.

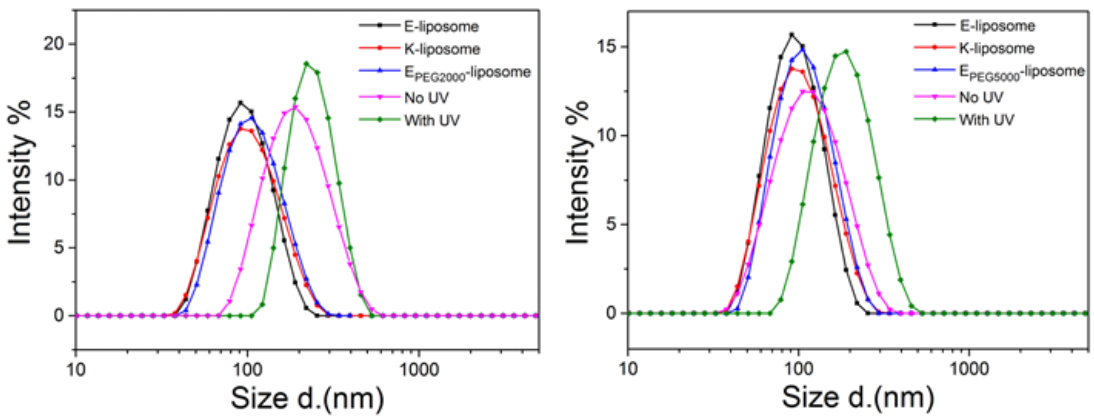

Figure S3 DLS data accompanying liposome-liposome lipid mixing experiments. For $E_{PEG2000}$-liposomes (left, 4 mol% PEG_{2000}) an increase in liposome hydrodynamic diameter was observed *in the absence* of UV irradiation/PEG photolysis. This indicates PEG_{2000} is not sufficiently long enough to shield E_4/K_4 recognition and binding. For $E_{PEG5000}$-liposomes (right, 4 mol% PEG_{5000}), an increase in liposome size is only observed following UV irradiation (15 mins, 370 ± 7 nm, 202 mW/cm^2), loss of PEG and restoration of the interaction between peptide E and K.

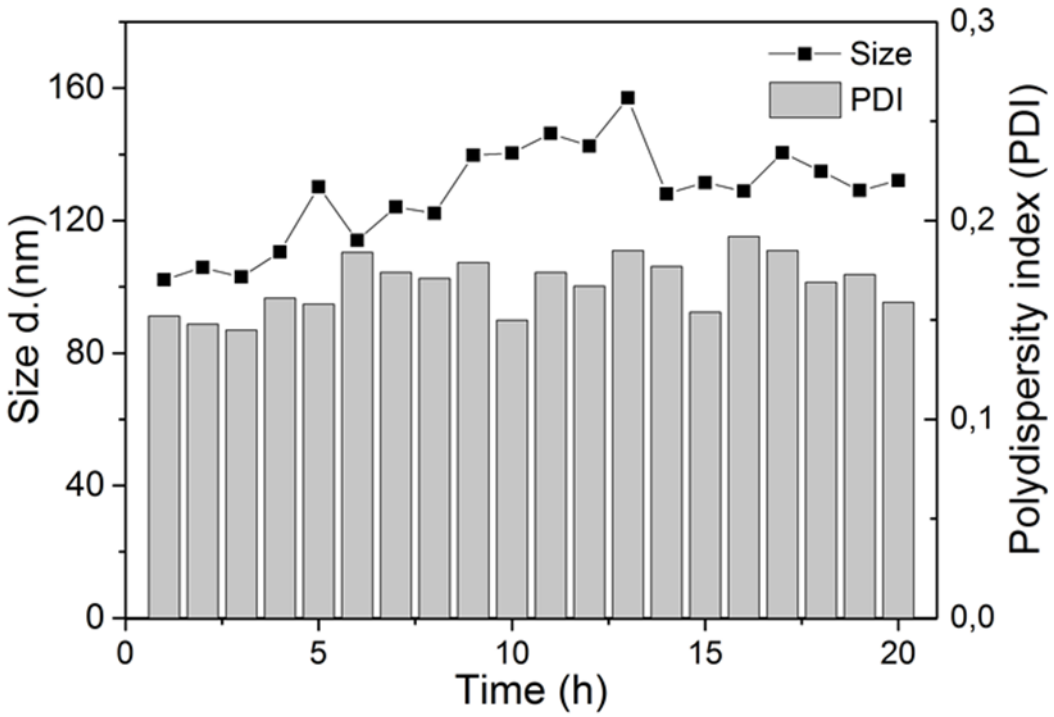

Figure S4 Stability of E_{PEG}-liposomes (4mol% PEG_{5000}) in media + 10% FCS over time

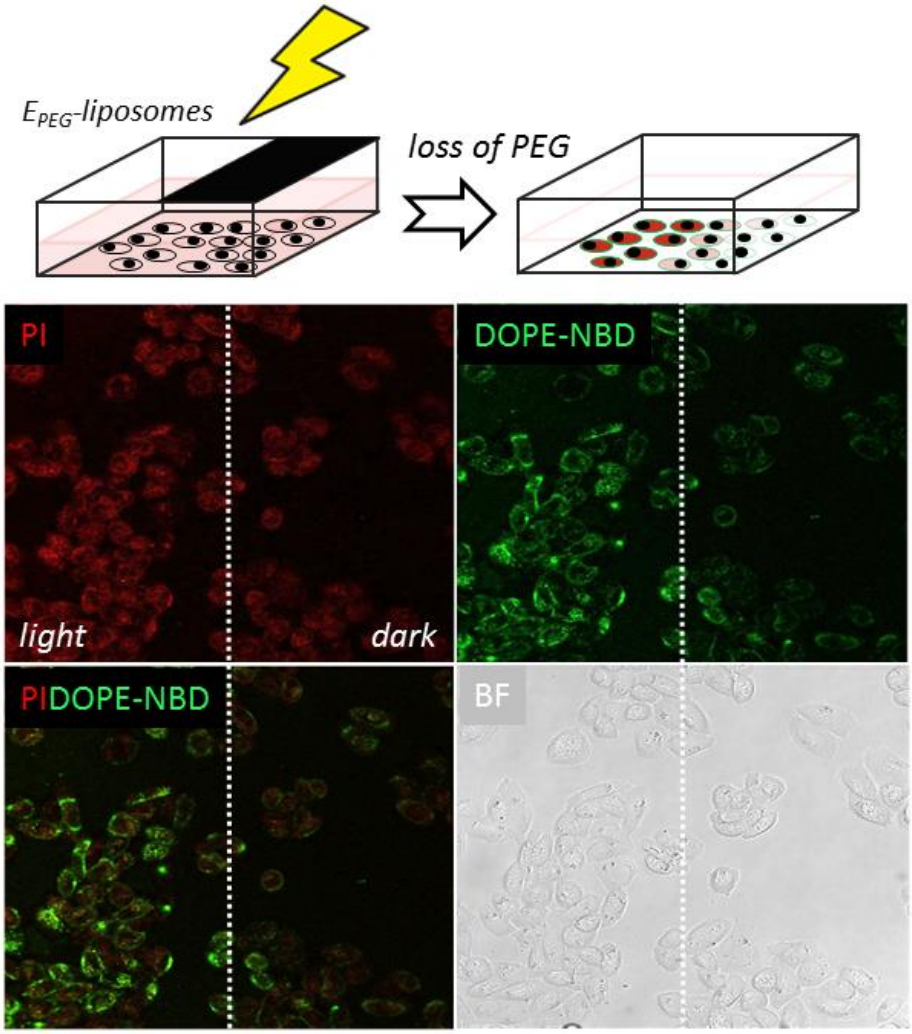

Figure S5 Light templated liposome-cell fusion and concomitant cargo delivery *in vitro*. Following localized UV irradiation (15 mins, 370 ± 7 nm, 50.6 mW/cm^2, *light dose* = 45.5 J/cm^2), E_{PEG}-liposomes (400 µM total lipids, 1 mol % DOPE-NBD, green lipid probe, 75 µM encapsulated PI, red) fuse with K-functionalized HeLa cell membranes with concomittant delivery of PI to the cell cytosol. In the absence of UV irradiation, but within the same experimental well, cells show significantly less liposome-associated fluorescence.

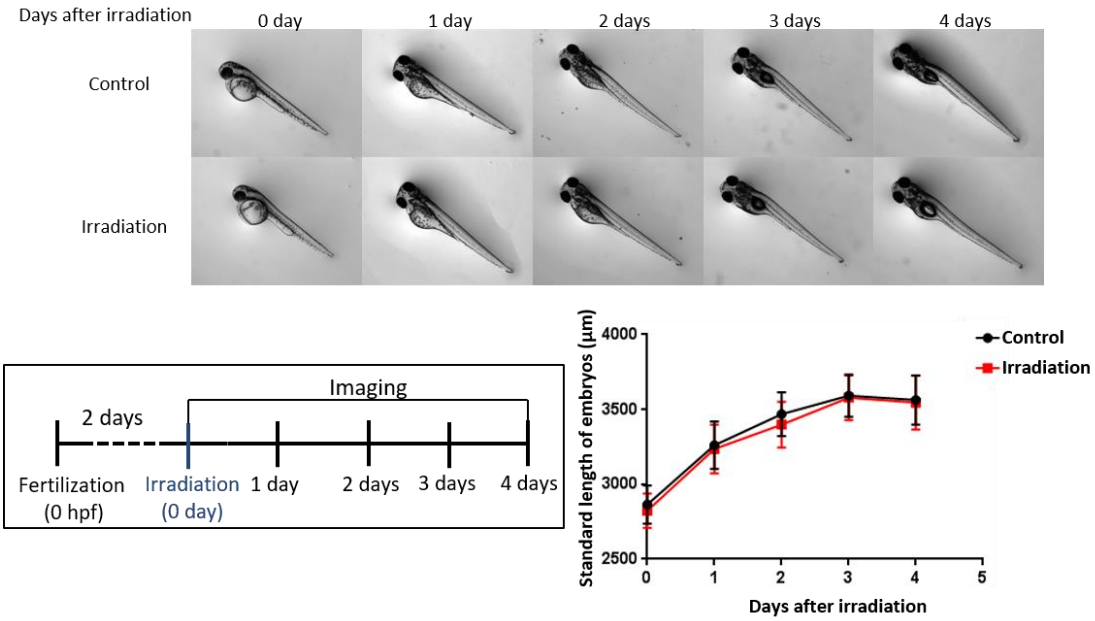

Figure S6 UV-A phototoxicity in zebrafish embryos. UV-A phototoxicity in zebrafish embryos. For irradiated embryos, a single dose of UV-A light (15 mins, 370 ± 7 nm, 13.5 mW/cm², *light dose* = 0.45 J/embryo) was applied to zebrafish embryos (2 dpf). Images were taken 0, 1, 2, 3, 4 days (2-6 dpf) after irradiation using a Leica MZ16FA fluorescent microscope (BF mode) coupled to a DFC420C camera. The standard length of embryos was measured from the eye to the end of the tail (ImageJ 1.51n). Under these irradiation conditions, embryos developed normally and no phenotypic abnormalities were observed. Data presented as mean ± SD. *Sample sizes*: Control group (d0: n = 20; d 1: n = 20; d2: n = 20; d3: n = 20; d4: n = 19) Irradiation group (d0: n = 20; d1: n = 19; d2: n = 18; d3: n = 18; d4: n = 16).

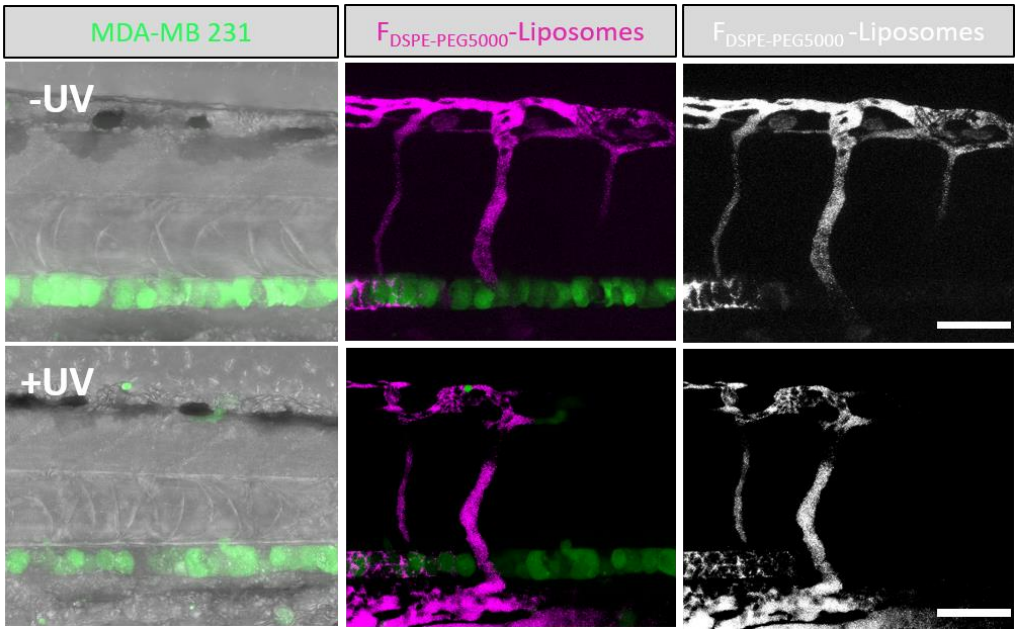

Figure S7 (Control for) Cell-specific, light triggered liposome-cell interactions *in vivo*. MDA-MB-231 human breast cancer cells, stably expressing GFP were injected into the circulation of a 2-day old zebrafish embryo and quickly accumulated in the caudal hematopoietic tissue (CHT). $F_{DSPE-PEG5000}$-liposomes (1 mM, 4 mol% DSPE-PEG_{5000}, containing 1 mol% DOPE-LR, red) were injected into circulation. In this case, both before and after UV irradiation (15 mins, 370 ± 7 nm, 13.5 mW/cm^2, *light dose* = 0.45 J/embryo), liposomes remained freely circulating, confined to the vasculature of the embryo. Scale bars = 100 µm

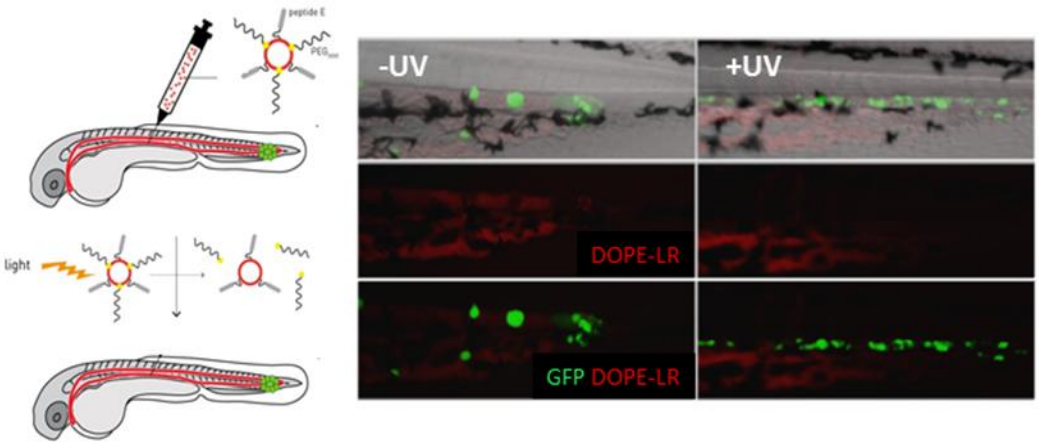

Figure S8 (Control for) Cell-specific, light triggered liposome-cell interactions *in vivo*. MDA-MB-231 human breast cancer cells, stably expressing GFP were injected into the circulation of a 2-day old zebrafish embryo and quickly accumulated in the caudal hematopoietic tissue (CHT). These cells had not been prior functionalized with lipopeptide K. E_{PEG}-liposomes (1 mM, 4 mol% PEG_{5000}, containing 1 mol% DOPE-LR, red) were injected into circulation. In this case, both before and after UV irradiation (15 mins, 370 ± 7 nm, 13.5 mW/cm^2, *light dose* = 0.45 J/embryo), liposomes remained freely circulating, confined to the vasculature of the embryo.

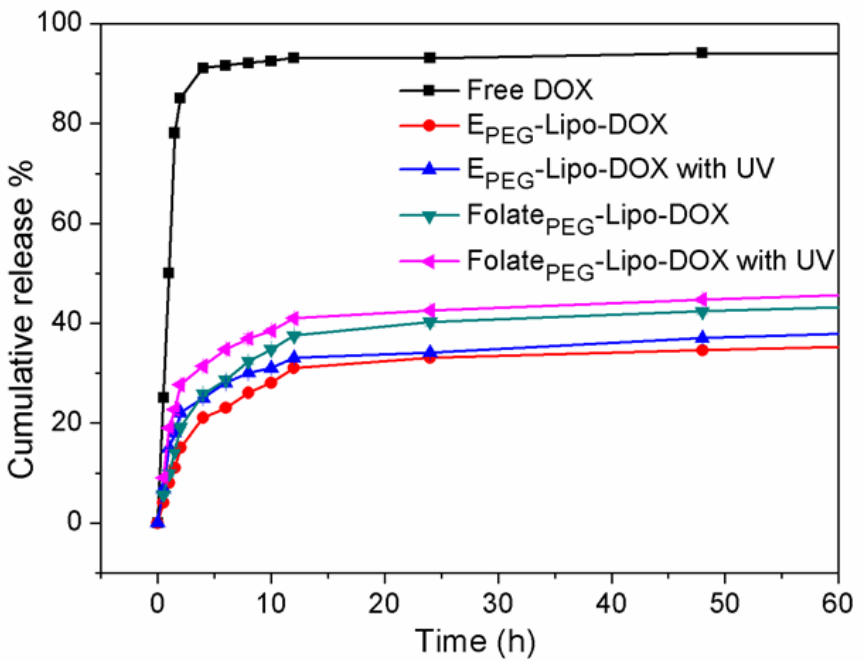

Figure S9 Doxorubicin release curves for E_{PEG}- and F_{PEG}-lipo-DOX formulations, before and after UV (15 mins, 370 ± 7 nm, 202 mW/cm^2) irradiation.

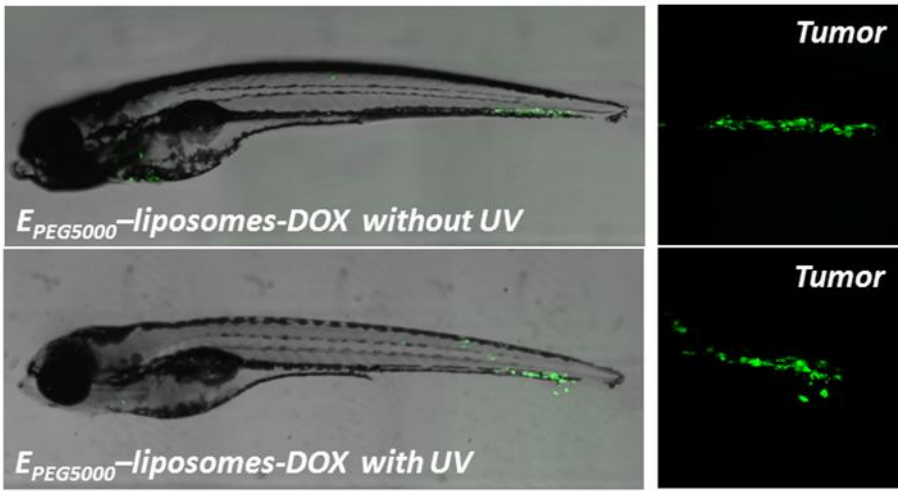

Figure S10 (Control for) Cell-specific doxorubicin delivery to xenograft cancer cells *in vivo*. MDA-MB-231 human breast cancer cells, stably expressing GFP were injected into the circulation of a 2-day old zebrafish embryo. These cells had not been prior functionalized with lipopeptide K. No reduction in tumor volume was observed following injection of doxorubicin-filled (200 µM doxorubicin) E_{PEG}-liposomes, both before (top) and after (bottom) *in situ* UV irradiation (15 mins, 370 ± 7 nm, 13.5 mW/cm^2, *light dose* = 0.45 J/embryo).